



MASTER THESIS

Wear Resistance, Mechanical Properties and Design Improvement for Lifetime of the Chain Parts

Mr. Perawat Thongjitr



A THESIS SUBMITTED IN PARTIAL FULFILLMENT OF THE REQUIREMENTS
FOR THE DEGREE OF MASTER OF ENGINEERING IN MATERIALS AND PRODUCTION ENGINEERING
THE SIRINDHORN INTERNATIONAL THAI-GERMAN GRADUATE SCHOOL OF ENGINEERING
KING MONGKUT'S UNIVERSITY OF TECHNOLOGY NORTH BANGKOK
ACADEMIC YEAR 2018

COPYRIGHT OF KING MONGKUT'S UNIVERSITY OF TECHNOLOGY NORTH BANGKOK

Author

Name	Mr. Perawat Thongjitr
Title	Wear Resistance, Mechanical Properties and Design Improvement for Lifetime of the Chain Parts
Major Field	Materials and Production Engineering
Advisor	Asst. Prof. Dr.-Ing. Pruet Kowitwarangkul
Academic Year	2018

Acknowledgement

First, I would like to thanks Asst. Prof. Dr.-Ing. Pruet Kowitwarangkul. Materials and Production Engineering Department for his guidance in this thesis project. And Thai Metro Industry (1973) Co., Ltd. for the opportunity to do the thesis. This thesis could not be achieved without their advice and support.

Secondly, I would like to thank the Innovation and Technology Assistance Program (ITAP), National Science and Technology Development Agency (NSTDA) Organizations that support the use of research funds.

Thirdly. I would like to thank Assoc. Prof. Siriporn Daopiset. The Department of Production Engineering (PE), CRDC, Institute for Scientific and Technological Research and Services (ISTRS), and Thai-German Institute (TGI) for support, testing and analysis of the experimental results.

Finally, I would like to give thanks to my family, friends and TGGs staffs for their help and assistance in this thesis project.

Perawat Thongjitr

Abstract

The aims of this thesis were to 1. investigate and improve the surface hardness and wear resistance of the pin parts and 2. analyze and prevent the cracking during usage of chain plate made from the V-Die Bending process by using computer simulation. Both methods result in lifetime extension of the roller chain used in an industrial factory and the agricultural industry.

In the first part of the thesis, the experiments were done by applying the carburizing and carbonitriding technique in the original heat treatment process of the example factory. Hardening agents were charged into the industrial rotary retort furnace. Hardened specimens from the experiments were investigated by Micro Vickers Hardness Test, Wear Test, Double Shear test, Scanning Electron Microscope (SEM) and Energy-Dispersive X-ray Spectroscopy (EDS) technique. The results show that the hardened specimens have better wear resistance property than the original product with an accepted shear strength and toughness.

The second part of the thesis was to prevent cracking of the chain plate in the corrosive condition. The computer simulation was used to examine to improve bending process design and to prevent the high stress concentration at the corner which leads to the formation of the cracking. The simulation results from the study defined the highest stress concentration occurred at the edge of the fillet of the original bending line 34 mm. The test results revealed that the simulation results are entirely consistent with the actual region of the cracking during usage. The new bending line 37 mm can reduce the stress concentration on the fillet zone of the chain plate.

Keyword: Heat treatment, Roller chain, V-Die bending, Wear resistance

Stress concentration

Table of contents

Author	i
Acknowledgement	ii
Abstract	iii
Table of contents	iv
List of figures	vii
List of tables	x
Nomenclature	xi
Chapter 1 Introduction	1
1.1. Background and Problem	1
1.2. Objectives of The Study	3
1.3. Scope of The Study	3
1.4. Utilization of The Study	3
Chapter 2 Theory and Literature Review	4
2.1. Roller Chain	4
2.1.1 Components of the Roller Chain	4
2.1.2 Effect of Chain Wear	5
2.2. Heat Treatment	6
2.2.1 Hardening Agent	7
2.2.2 Carburization	9
2.2.3 Carbonitriding	10
2.2.4 Decarburization	11
2.2.5 Phase Transformation	11
2.3. Testing	13
2.3.1 Hardness Tests	13

2.3.2	Double Shear Test.....	14
2.3.3	Charpy Impact Test.....	15
2.3.4	Wear Mechanism	16
2.4.	Sheet Metal Forming	18
2.4.1	V-Die Bending.....	19
2.4.2	Stress Concentration	19
2.4.3	Application in FEM	20
2.4.4	Computer Simulation.....	20
2.4.5	Residual stress.....	21
2.4.6	Corrosion.....	22
Chapter 3	Experimental Procedure	23
3.1.	Heat Treatment Process	23
3.1.1	Material	23
3.1.2	Furnace.....	24
3.1.3	Hardening Agent.....	24
3.1.4	Heat Treatment.....	26
3.2.	Characterizations	30
3.2.1	Hardness Test.....	30
3.2.2	Charpy Impact Test.....	31
3.2.3	Dry Sliding Wear Test	31
3.2.4	Double Shear Test.....	32
3.2.5	Microscopy	33
Chapter 4	Results and Discussion.....	34
4.1.	11 mm Pin Diameter.....	34
4.1.1	Internal Results (Measured in the Factory).....	34
4.1.2	Micro Vickers Hardness Test.....	36
4.1.3	Double Shear Test.....	39
4.1.4	Wear Test	40
4.1.5	Microstructure.....	42

4.1.6	Discussion	45
4.2.	9.5 mm Pin Diameter	46
4.2.1	Internal Results	46
4.2.2	Double Shear Test.....	47
4.2.3	Wear Test	48
4.2.4	Discussion	49
4.3.	5.9 mm Pin Diameter	50
4.3.1	Internal Result	50
4.3.2	Wear Test	51
4.3.3	Discussion	52
4.4.	Discussion.....	52
4.5.	Future Work.....	53
Chapter 5	Computer Simulation	54
5.1.	Background and Problem	54
5.2.	Simulation Setup	56
5.2.1	Geometry Module	57
5.2.2	Connection Module.....	57
5.2.3	Mesh Module	58
5.2.4	Initial Conditions Module	59
5.3.	Simulation Results.....	60
5.4.	Validation	63
5.5.	Discussion.....	67
5.6.	Future Work.....	67
Chapter 6	Conclusion.....	68
Bibliography	71
Biography.....		78
Appendix A.....		80
Appendix B		88
Appendix C.....		91

List of figures

Figure 1.1 Assembly of roller chain	1
Figure 1.2 The surface contact between pin and bush.....	2
Figure 2.1 The Components of Roller Chain [5]	4
Figure 2.2 The Disintegration of Ammonia [20].....	9
Figure 2.3 Isothermal Transformation Diagram for an Alloy Steel (type 4340): A, Austenite; B, Bainite; P, Pearlite; M, Martensite; F, Ferrite [29].....	12
Figure 2.4 Rockwell Hardness Test.....	14
Figure 2.5 Principal of the Vickers Hardness Test	14
Figure 2.6 Double Shear Test	15
Figure 2.7 Charpy Impact Test	16
Figure 2.8 Wear Test.....	18
Figure 2.9 V-Die Bending: description of a process.....	19
Figure 2.10 Stress Concentration Factor for Rectangular Plate with Fillet (Bending Load).....	20
Figure 3.1 Dimension of Specimen	23
Figure 3.2 Rotary Retort Furnace	24
Figure 3.3 Charcoal Powder to be used as a Hardening Agent	25
Figure 3.4 Iron-carbon phase diagram [60]	26
Figure 3.5 The Heat Treatment Process.....	27
Figure 3.6 Measurement Position of Specimen	30
Figure 3.7 Vickers Hardness Test (A) Measurement Positions, (B) Points on The Specimen.....	30
Figure 3.8 Charpy Impact Test Machine	31

Figure 3.9 Dry Sliding Wear Test (A) Tribology Testing Machine, (B) Cross-section Area Measured by the Profilometer	32
Figure 3.10 Double Shear Test (A) Machine and Specimen Holder Equipment, (B) Double Shear Test Result.....	33
Figure 3.11 Scanning Electron Microscopy.....	33
Figure 4.1 Hardness Profile of Original Product	37
Figure 4.2 Hardness Profile of Experiment CA-01	37
Figure 4.3 Hardness Profile of Experiment CA-02	37
Figure 4.4 Hardness Profile of Experiment CB-01.....	38
Figure 4.5 Hardness Profile of Experiment CB-02.....	38
Figure 4.6 Hardness Profile of Experiment CN-01	38
Figure 4.7 Hardness Profile of Experiment CN-02	38
Figure 4.8 Micro Vickers Hardness at the Edge	38
Figure 4.9 The Results from Double Shear Test (A) Shear Strength, (B) Maximum load and (C) Toughness of The 11 mm Diameter	40
Figure 4.10 Wear Loss Area (A) after 15 minutes, (B) after 30 minutes of The 11 mm Pin Diameter	41
Figure 4.11 Wear Loss Area (A) after 15 minutes, (B) after 30 minutes of The Experiment Specimens and other products.....	42
Figure 4.12 Microstructure of The Original Product (A) at the edge and (B) at the center	43
Figure 4.13 Microstructure of the Experiment Specimens in Carburizing Process (code CA, CB) (a) at the Edge and (b) at the Center	43
Figure 4.14 Microstructure of the Experiment Specimens in Carbonitriding Process (code CN) (A) at the Edge and (B) at the Center.....	44
Figure 4.15 The Results from Double Shear Test (A) Shear Strength, (B) Maximum Load, and (C) Toughness of The 9.5 mm Pin Diameter	48
Figure 4.16 Wear Loss Area (A) after 15 minutes, (B) after 30 minutes of The 9.5 mm Pin Diameter	49

Figure 4.17 Wear Loss Area (A) after 15 minutes, (B) after 30 minutes of The 5.9 mm Pin Diameter	52
Figure 5.1 Cracking caused Chain Fracture after Usage	55
Figure 5.2 Bending line of Chain Plate at 34 mm (PH-A) and 37 mm (PH-B).....	56
Figure 5.3 Simulation Setup in ANSYS 18.1 Program	56
Figure 5.4 (A) Model for Simulation, (B) Sizing of Meshing in Simulation	59
Figure 5.5 The Computer Simulation Result of PH-A (A) Von-Mises Stress, and (B) Maximum principal Stress	60
Figure 5.6 The Computer Simulation Result of PH-B (A) Von-Mises Stress, and (B) Maximum principal Stress	61
Figure 5.7 The Comparison between (A) The Original Bending line, and (B) The New Bending line	61
Figure 5.8 The Measurement Positions of the Specimen	62
Figure 5.9 Stress Profile from Bending Simulation between PH-A and PH-B (A) Von Mises Stress and (B) Maximum principal Stress.....	63
Figure 5.10 Micro Vickers Hardness Test	63
Figure 5.11 Validation of the Computer Simulation with Micro Vickers Hardness Test near the Fillet Zone	64
Figure 5.12 Validation between Computer Simulation Result and Lab Test of Specimen (A) the Original Bending line (34 mm) and (B) the New Bending line (37 mm)	65
Figure 5.13 The Comparison of Bending Process Results between (A) the Computer Simulation, and (B) the Bending Machine (34 mm).....	66
Figure 5.14 The Comparison of Bending Process Results between (A) the Computer Simulation, and (B) the Bending Machine (37 mm).....	66

List of tables

Table 2.1 The Surface hardness of roller chain parts standard [5]	5
Table 2.2 Chemical Reactions related to the Hardening Agents [12].....	7
Table 3.1 Chemical Composition	23
Table 3.2 Hardening Agents in the Experiments	25
Table 3.3 Results from Analyzed Hardening Agent.....	26
Table 3.4 The Test Conditions of the Experiment.....	29
Table 3.5 Test Condition of Wear Test.....	32
Table 4.1 The Internal Results	34
Table 4.2 The Results from Double Shear Test.....	39
Table 4.3 The Result from Tribology Testing	40
Table 4.4 The Results from Energy-Dispersive X-ray at the Edges and Center	44
Table 4.5 The internal results.....	46
Table 4.6 The Results from Double Shear Test.....	47
Table 4.7 The Results from Tribology Test.....	48
Table 4.8 The internal results.....	50
Table 4.9 The Results from Tribology Test.....	51
Table 5.1 The Setup in Geometry Module.....	57
Table 5.2 The Setup in Connection Module	58
Table 5.3 The Setup in Mesh Module.....	58
Table 5.4 The Setup in Transient Module	59
Table 5.5 The Results from Vickers Hardness Test and Simulation	64

Nomenclature

A	Area [m^2]
d_1	Indent diagonal
d_2	Indent diagonal
E	Modulus of elasticity [N/mm^2]
F	Force [kgf]
F_{max}	Maximum force [N]
F_N	Normal load [N]
HV	Vickers hardness test [HV]
K	Diffusivity constant
K_t	Stress concentration factor
W_s	Specific wear rate
S_s	Sliding distance [mm]
ΔV	Volume loss [mm^3]
σ	Stress [N/mm^2]
σ_{avg}	Average normal stress [N/mm^2]
σ_{max}	Maximum stress [N/mm^2]
σ_y	Yield stress [N/mm^2]
τ	Shear stress [N/mm^2]
δ	Modulus of elasticity

Chapter 1 Introduction

1.1. Background and Problem

The roller chain is the most used power transmission equipment in industry. The roller chain is the component in the machine for transmission, conveyor and agriculture. The function of the roller chain is the power transmission from driver to the pinion gear according to the motion. The components of roller chain are pin, bush, roller, pin link plate and roller link plate as shown in Figure 1.1. The manufacture of roller chains has been standardized by the American National Standards Institute under standard B29.1 [1]. The mechanical properties of the component parts of chain are very important because it is related to the chain performance, the specification, the wear and accumulated elongation during using. This study has been carried out at Thai Metro Industry (1973) Co., Ltd. which is one of the roller chain manufacturers in Thailand.

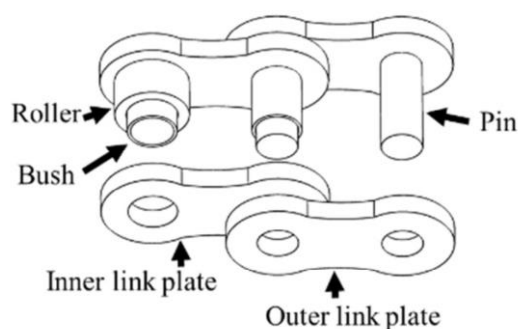


Figure 1.1 Assembly of roller chain

The first part of this thesis is to investigate and improve the surface hardness and wear resistance of the pin through the heat treatment process, which will extend the lifetime of the chain. At the same time, the other material properties, e.g., toughness and shear strength were also investigated and controlled to meet the specification of the company. Normally, a roller chain enters and leaves the sprockets during usage and the

wear take place at the surface contact between the pin and bush as shown in Figure 1.2. As material is worn away from these surfaces the roller chain will gradually elongate [2] and finally results in the expiry of chain lifetime.

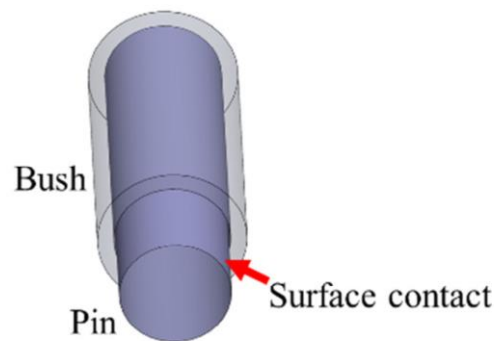


Figure 1.2 The surface contact between pin and bush

In the production of a roller chain, each component is usually heat treated to improve the mechanical properties. During this process, decarburization can take place at the surface of the steel components. With the low carbon content at the surface of the pin specimen, it can cause a problem, as the weaker surface layer reduces wear resistance, enabling fatigue failures to occur more easily [3]. In many engineering applications, a steel part is needed to have a hardened surface for wear resistance. At the same time, high toughness inside materials are required in order to absorb any shock load [4]. The experimental procedure and the results of wear resistance improvement of the pin parts are shown in Chapter 3 and Chapter 4 respectively.

Furthermore, the cracking during usage of the chain plate and the distribution of stresses in the bending line were also investigated in Chapter 5, the later part of this study. The V-die bending process of the roller chain plate was examined to prevent cracking, resulting in an increased lifetime extension of the chain plate by using computer simulation.

The aims of the research were to improve the lifetime of the roller chain used in an industrial factory and the agricultural industry, also to enhance the quality of the products in order to gain acceptance of the customers.

1.2. Objectives of The Study

1. To investigate and improve the surface hardness and wear resistance of the roller chain parts, which will result in the lifetime extension.

2. To analyze and prevent the cracking during usage of the chain plate made from the V-die bending process by using computer simulation.

1.3. Scope of The Study

1. The testing specimens are pin and chain plate of roller chain which is made from 0.4% C Steel (SNCM 439 and SCM 435). The diameter of pins are 5.9, 9.5 and 11 mm.

2. In this study the carburizing and carbonitriding techniques are applied in the original heat treatment process at Thai Metro Industry (1973) Co., Ltd. The hardening agents are the mixture of charcoal, BaCO_3 and Urea in solid state. The parameters of the experiments are the composition and mass of the mixture and heat treatment period. The investigated properties are microstructure, hardness, shear strength and wear.

3. The computer simulation of V-die bending process is used to analyze the stress concentration in the chain plate during V-die bending process. The simulation will be done in different conditions by changing the position of V-bend on the plate.

1.4. Utilization of The Study

The results from the first part of the research will show how to improve mechanical properties of the roller chain parts by the heat treatment process. The computer simulation in the second part of the research will help to improve bending process design and prevent the high stress concentrations at the corner which lead to the initiation of the cracking. Both results will offer the solutions that will help the factory to increase the lifetime of the roller chain parts.

Chapter 2 Theory and Literature Review

2.1. Roller Chain

The roller chain is the component in a machine that is most used for power transmission equipment in industry. The functions of the chain are mainly used for power transmission. The components of roller chain are shown in Figure 2.1.

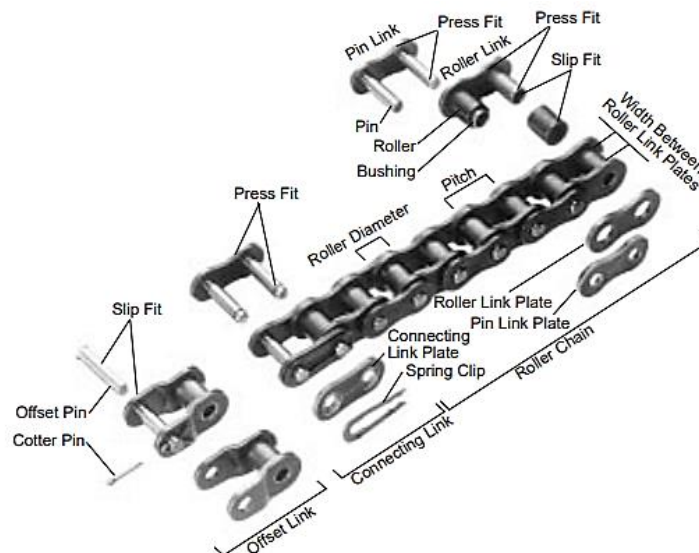


Figure 2.1 The Components of Roller Chain [5]

Sachio Shimura explained the function and relationship of each component of the roller chain as follows:

2.1.1 Components of the Roller Chain

1. There are two types of the chain plate: 1. Pin Link Plate and 2. Roller Link Plate. The plates of the roller chain are the component that absorbs the tension force and are sometimes accompanied by shock. The plate must have the properties environmental resistance.

2. The bushing is absorbing the shearing and bending forces transferred by the plate and roller. When the chain articulates, the inner surface contact with pin and the outer surface contact with roller. Therefore, the bush must have good tensile strength to absorb the load.

3. The roller is absorbing the impact load from contact with the sprocket. The roller chain moves between the sprockets while receiving a compression load. Furthermore, the roller's inner surface contact with the outer surface of the bush. Therefore, it must be resistant to wear and high strength compression.

4. The pin is absorbing the shearing and bending forces transferred by the plate. At the same time, when the chain is flexible during the contact of the sprocket. Therefore, the pin needs to be high tensile and have shear strength, and also must have good wear resistance.

2.1.2 Effect of Chain Wear

The factors that affect the chain wear are very complicated. There are many considerations, such as lubrication, assembly accuracy, condition of produced parts, and the method of producing parts; therefore, wear value can't be greatly improved by merely changing one factor.

In transmission chains, JIS B 1801-1990 regulates the surface hardness of the pin, the bushing, and the roller as shown in Table 2.1 to meet the multiple requirements for wear resistance and shock resistance [5].

Table 2.1 The Surface hardness of roller chain parts standard [5]

Component	HV	HRC
Pin	450 or greater	45 or greater
Bush	450 or greater	45 or greater
Roller	390 or greater	40 or greater

2.2. Heat Treatment

Temperature, time, and hardening agent have a significant influence on the heat treatment process. Heat treatment can affect the strength of a metal or increase its toughness. Wear resistance in a metal is heavily affected by heat treatment [6].

The importance of heat treatment operations on medium carbon steel may create a problem from faulty heat treatment operations which can cause failure of the machine components. Many research studies showed that the mechanical properties depend largely upon the various forms of heat treatment operations and the cooling rate. The mechanical properties and the applications modified by heat treating the medium carbon steel in order to make it suitable to the purpose [7].

A previous study of Hardness Improvement on Low Carbon Steel using Pack Carbonitriding Method with Holding Time Variation applying a newly innovated method of pack carbonitriding using charcoal and urea showed that carbonitriding temperature difference affect the mechanical properties of steel. The study showed that longer holding time in a certain temperature and higher austenite can affect the mechanical properties of the specimen [8].

Aramide et al. carried out an experiment on the effects of the carburizing temperature and time on the mechanical properties of mild steel carburized with activated carbon at temperatures of 850, 900, 950°C with soaking time of 15 and 30 min. It was found that despite the short interval of soaking time, the result showed an improvement in the case depth and other mechanical properties of the mild steel [9].

The carburization process decreases the impact energy (toughness) of the mild steel. And the toughness is decreased with an increase in the carburization temperature. The stiffness of the mild steel is increased by the carburization process, but it decreases with increasing the carburizing temperature. The carburization treatment followed by the oil quenching and tempering at 550°C strongly influence the hardness and tensile strength of mild steels [10].

Paul Aondona Ihom [11] studied various carburizing compounds were used to pack carburized mild steel. In his study various weight percentages of cow bone were used as energizer in the carburizing compounds. The experiment was carried out using a muffle furnace at 900°C for 8 h. The result showed that 60 wt% charcoal with 40 wt% cow bone had the best result with an effective case depth of 2.32 mm produced on the case of the carburized steel. The work showed that cow bone can be used as an energizer in pack carburization of mild steel.

2.2.1 Hardening Agent

In this study, a small amount of charcoal was charged at the beginning of the heat treatment process as a reducing agent to reduce oxygen of the atmosphere inside the furnace and to prevent oxidation of the steel product. Some amounts of barium carbonate (BaCO_3) are charged together with charcoal to promote the Boudouard Reaction. In the experiments, the different mixtures of charcoal+ barium carbonate both with and without adding the urea were charged during the heat treatment process as a hardening agent to perform carburizing and carbonitriding reactions [12] at the surface of the specimens. The chemical reactions related to the hardening agents are shown in Table 2.2.

Table 2.2 Chemical Reactions related to the Hardening Agents [12]

Hardening agent	Chemical reactions
Charcoal	$\text{C} + \text{CO}_2 \rightarrow 2\text{CO}$
Barium carbonate	$\text{BaCO}_3 \rightarrow \text{BaO} + \text{CO}_2$
Urea	$(\text{NH}_2)_2\text{CO} \rightarrow \text{NH}_3 + 0.5\text{H}_2 + 0.5\text{N}_2 + \text{CO}$

Charcoal is defined as carbonized wood used mainly as fuel or as a reductant in industry, e.g., to reduce oxidized iron ores in iron and steel production [13]. Charcoal is mostly pure carbon, made by cooking wood with low oxygen. The process can take

days and burns off volatile compounds such as water, methane, hydrogen, and tar, and leaving about 25% of the original weight in black lumps and powder. Regarding quality of charcoal, better chemical properties of charcoal are reached with higher levels of fixed carbon and lower levels of ash and volatiles. Thus, charcoal has a relatively low moisture content of around 5 to 15%. The volatile matter [14] and the ash content are linked to the amount of fixed carbon. High quality charcoal should have the fixed carbon content of about 75% and the final carbonization temperature of around 400-500°C [15]. Carbon is the main hardening element in all steel. The strengthening effect of C in steels consists of solid solution strengthening and carbide dispersion strengthening. As the C content in steel increases, strength increases, but ductility and weldability decrease [16].

Barium Carbonate (BaCO_3) is the principal energizer, usually comprising about 50 to 70% of the total carbonate content. It is one of the energizers used in carburization. The remainder of the energizer is usually made up of calcium carbonate and sodium carbonate [17].

Urea ($\text{CO}(\text{NH}_2)_2$) is a solid product in the shape of grains; its main characteristic is N in the form of an amide (NH_2). The compound is commercially synthesized by a reaction of ammonia (NH_3) and carbon dioxide (CO_2) under conditions that are dependent on the technology employed in the industrial plant [18]. Svetlana Bashkova et al. studied the removal of NO_2 on urea-modified and heat-treated wood-based activated carbons. It was found that urea supported on activated carbon effectively reduced both NO_2 and NO to N_2 and the reduction continued until the complete consumption of urea [19]. Nitriding from nitrogen content contained in urea occurs after the disintegration of ammonia [8]. Nitrogen atoms diffuse to the surface of the steel, as shown in Figure 2.2.

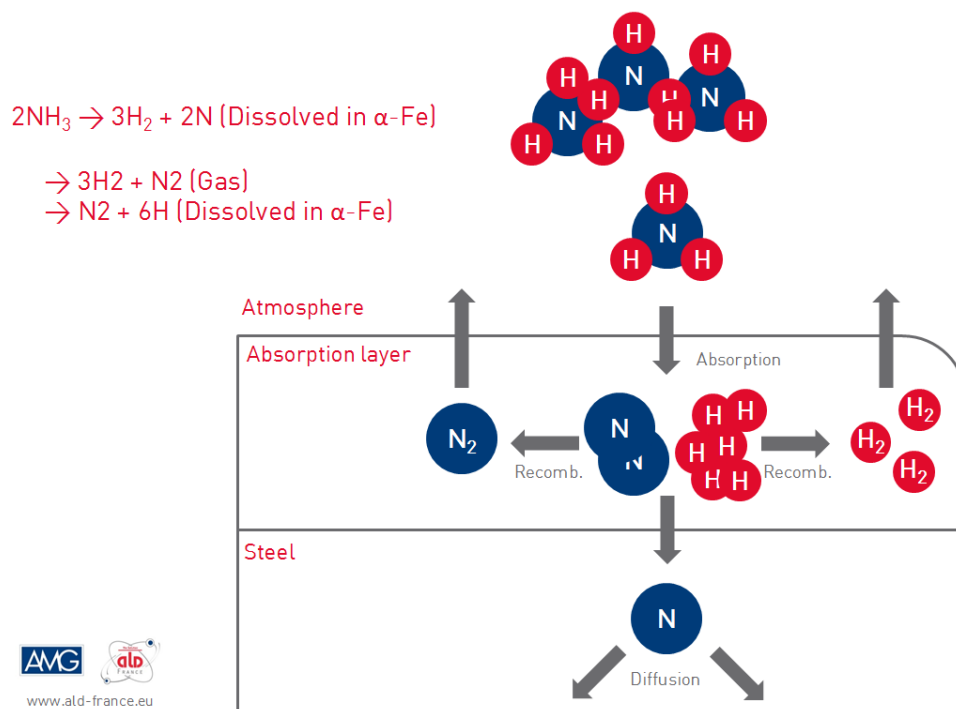


Figure 2.2 The Disintegration of Ammonia [20]

The basic process used is thermochemical because some heat is needed to enhance the diffusion of hardening elements into the surface and subsurface regions of a part. The depth of diffusion exhibits a time temperature dependence. Concentration gradients depend on the surface kinetics and reactions of a particular process. The diffusivity constant, K , depends on temperature, the chemical composition of the steel, and the concentration gradient of a given hardening element [21].

$$\text{Case depth} = K\sqrt{\text{Time}} \quad (2.1)$$

2.2.2 Carburization

Pack carburization or solid carburization uses solid carburizing material as the carbonaceous source. Commercial pack carburization utilizes energizers in the case hardening of mild steel. Different types of energizers are used together with carbonaceous materials to increase the carbon potential of carburizing materials. Carburizing performance depends on the effective control of the three principals variables: temperature, time and the carburizing atmosphere [22]. The commonly used

energizers are BaCO_3 , Na_2CO_3 , and CaCO_3 [11]. Pack carburization of steel parts is conventionally carried out at about 850 °C to 950 °C using carburizing compounds made up of charcoal and an energizer (a catalyst), traditionally barium carbonate. The energizer which usually amounts to some 6-20% of the compound is supposed to breakdown in the presence of carbon to form the active CO thus:



The CO then breaks down at the steel surface according to the reverse of the reaction (2.3) above i.e.



The oxide of the energizing compound in turn reacts with CO_2 liberated in Equation (2.4) to reform the carbonate. While the carbon is readily dissolved by the austenite phase of the steel and diffuses into the steel which upon subsequent quenching develops a hard case [23]. The higher the carbon potential the higher the equilibrium carbon concentration at the surface of the steel and thus the deeper the carburizing depth.

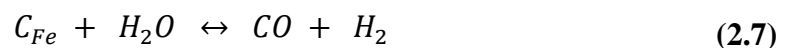
2.2.3 Carbonitriding

Carbonitriding is a surface-hardening heat treatment that introduces carbon and nitrogen into the austenite of steel. This treatment is similar to carburizing in that the austenite composition is changed and high surface hardness is produced by quenching to form martensite. However, because nitrogen enhances hardenability, carbonitriding makes possible the use of low-carbon steel to achieve surface hardness equivalent to that of high-alloy carburized steel without the need for drastic quenching, resulting in less distortion and minimizing the potential for cracks [21].

2.2.4 Decarburization

Decarburization is a significant problem in the heat treatment of steels as decarburization is detrimental to wear life and fatigue life of components [24]. Decarburization, as the term implies, is a loss of carbon atoms from the surface of the specimen, thereby producing a surface with a lower carbon content compared to a short distance beneath the surface. If carburization promotes a positive carbon gradient, then decarburization promotes a negative carbon gradient. The useful properties developed by carburizing and hardening will not be realized if the working surface of the component becomes decarburized, which frequently occurs in steel exposed to air at high temperature, resulting in loss of hardness at the surface [25].

Decarburizing reactions can occur at temperatures above about 700 °C and when, in the furnace atmosphere, decarburizing agents are available to react with the carbon in the metal surface [26]. The decarburizing agents used in furnace atmospheres for carburizing and reheating are carbon dioxide (CO₂), water vapor (H₂O), hydrogen (H₂), and oxygen (O₂). Under certain conditions, these gaseous molecules can react with the carbon atoms at the gas-metal interface and thereby extract them from the surface of the metal. This extraction is an attempt to establish some measure of equilibrium between the gas and metal. The chemical reactions involved are:



2.2.5 Phase Transformation

The transformation from austenite to martensite proceeds as the temperature is reduced below martensite start (M_s) until the martensite finish temperature (M_f) is reached, at which point 100% martensite is expected. However, if the M_f temperature is below room temperature, then some austenite may be retained if only cooled to room

temperature. Conversely, retained austenite can become stable if a part with a high-carbon surface layer [27] is quenched to about room temperature, held there for some time, and then refrigerated to below the M_f , some of the austenite will transform isothermally to martensite and some will survive. This surviving austenite is referred to as thermally stabilized austenite, and it requires a fair amount of energy to destabilize it [28].

Martensite is a nonequilibrium single-phase structure that results from a diffusionless transformation of austenite [29] as shown in Figure 2.3. Martensite is formed when austenitized iron-carbon alloys are rapidly cooled (or quenched) to a relatively low temperature.

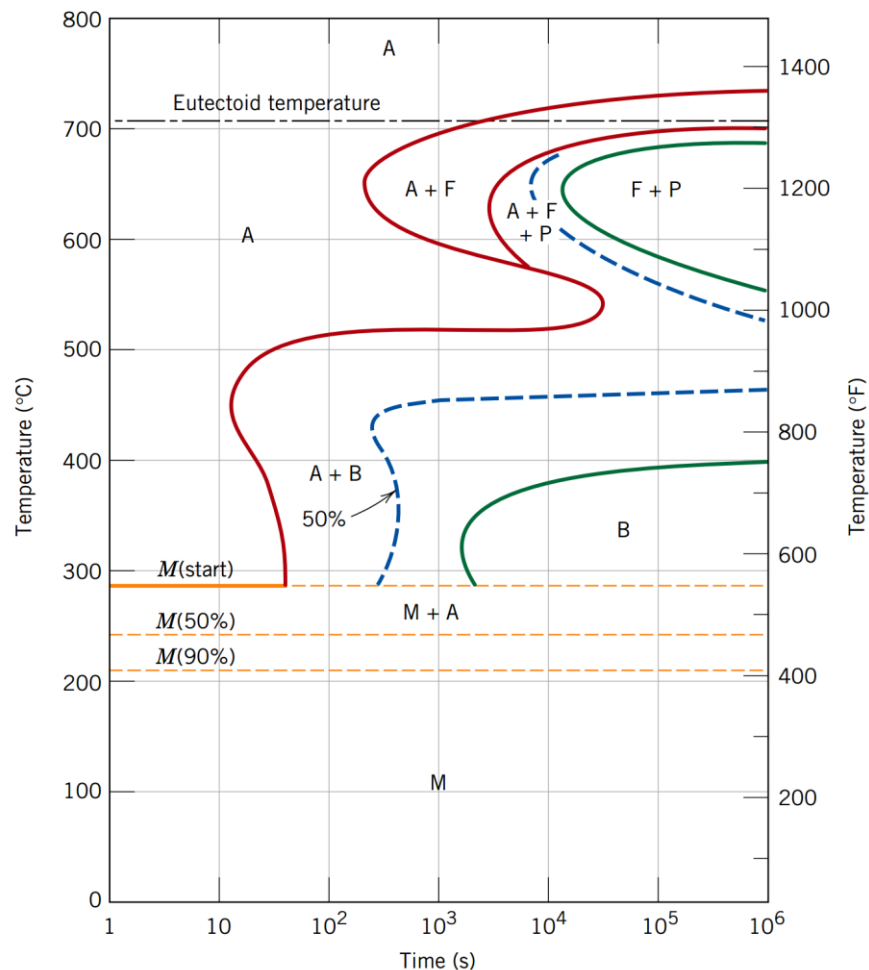


Figure 2.3 Isothermal Transformation Diagram for an Alloy Steel (type 4340): A, Austenite; B, Bainite; P, Pearlite; M, Martensite; F, Ferrite [29]

2.3. Testing

The mechanical properties of materials indicate their behavior under applied loads. Specifically, the mechanical behavior of a material characterizes. Mechanical properties include stiffness, strength, ductility and hardness [30].

2.3.1 Hardness Tests

Hardness is defined as resistance of a material to penetration of its surface. Most indentation hardness tests are a measure of the deformation that occurs when the material under test is penetrated with a specific type of indenter [31]. A definite value is obtained as the hardness of the metal, and this number can be related to the tensile strength of the metal [32].

a.) Rockwell hardness is probably the most used hardness testing method because it is simple and self-contained, there is no need for a separate microscope reading, and its values have a lot of meaning for practicing mechanics; it has scales (Rockwell A, Rockwell B, etc.) for different hardness ranges. A small-diameter steel ball is used as the indenter for soft materials, and a diamond cone for hard materials. The depth of penetration is measured automatically by the testing machine and converted to a Rockwell hardness number. Therefore, each measurement requires only a few seconds. For each scale, hardness values range up to 100. The theory and practice of Rockwell Testing is most authoritatively exposed in: ASTM E 18 - Standard Test Method for Rockwell Hardness and Rockwell Superficial Hardness of Metallic Materials. An International standard, issued by ISO – International Standards Organization is also available: ISO 6508-1 Metallic Materials - Rockwell Hardness Test. The indenter is either a "spheroconical" diamond (called "Brale") shaped in conical form, with an included angle of 120 degrees and with a smoothly rounded tip of 0.2 mm radius, or a hardened ball of one of a range of different diameters (1/16", 1/8", 1/4", 1/2") [33] as shown in Figure 2.4.

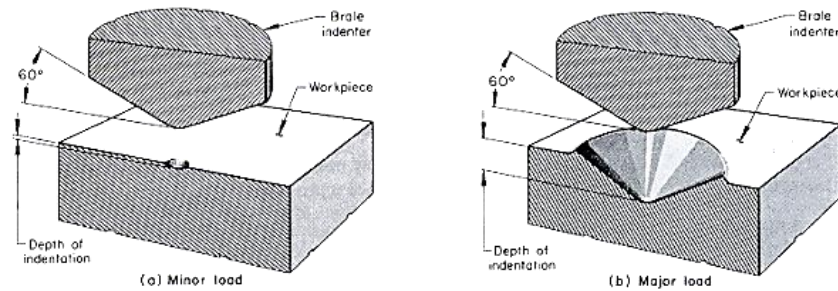


Figure 2.4 Rockwell Hardness Test

b.) The Vickers Hardness Test is the method most often used. Hardness can be from around 3 HV (soft metals) to 1500 HV (hard metals). This method is especially well suited for very hard materials and for small or thin samples. Hardness testing after Vickers (DIN EN ISO 6507). The test area A is the area of the diamond, i.e. the four faces of the pyramid, which penetrates into the material as shown in Figure 2.5. There is, however, a simple relationship between this area and the diagonals d . (F = test force, d_1, d_2 = indent diagonals). Vickers hardness is given in HV and calculated as test force / test area [30].

$$HV = \frac{1}{9.81} \times \frac{F}{A} \quad (2.9)$$

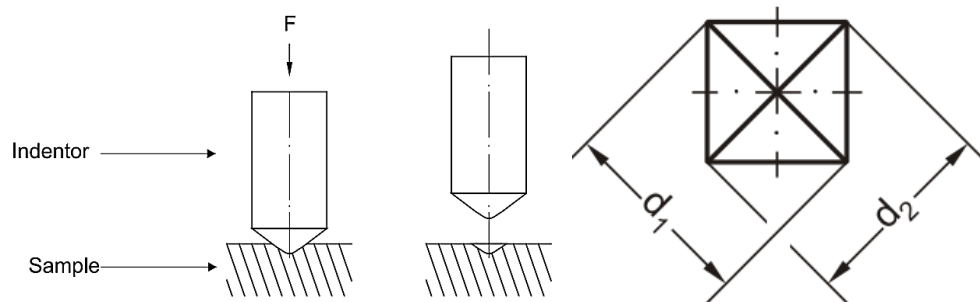


Figure 2.5 Principal of the Vickers Hardness Test

2.3.2 Double Shear Test

Direct Shear Stress and Test Mechanical joints, such as rivets, bolts, and pins, often experience direct shearing stress, which is defined as the shearing force divided by the cross-sectional area of the rivet, bolt, or pin [34].

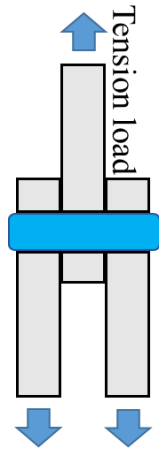


Figure 2.6 Double Shear Test

The shear strength of a joint is determined by a shear test in which the joint is usually subjected to double-shear loading (Figure 2.6). The load required to fracture the joint is determined, and the shear strength is calculated from where τ is the maximum shear strength, F is the shear force and A is the cross-sectional area. Equation (2.9) gives the average shear stress. The specimens that resist shearing forces at a single cross section are called single shear joints, and those resisting shearing forces at two cross sections are called double-shear joints [35].

$$\tau = \frac{F_{\max}}{2A} = \frac{F_{\max}}{2(\pi d^2/4)} = \frac{2F_{\max}}{\pi d^2} \quad (2.10)$$

2.3.3 Charpy Impact Test

The Charpy Impact Test is the most often used method to determine toughness. The reasons for this are that it has cost effective sample production and simple experimental procedures. The Charpy impact test is the most favorable method for determining absorbed energy (Figure 2.7). The tougher steels absorb more energy, whilst brittle materials tend to absorb significantly lesser energy prior to a fracture. The Charpy test also has standardized experimental procedures. The results for the minimum notch impact toughness at certain temperatures are used as a classification criterion in many steel production facilities. However, several disadvantages result from the simplicity of the test: Only qualitative parameters can be determined, i.e. the

determined parameters are dependent on the geometry and cannot be directly applied to components of the same material. Only different materials can be compared with one another [30].

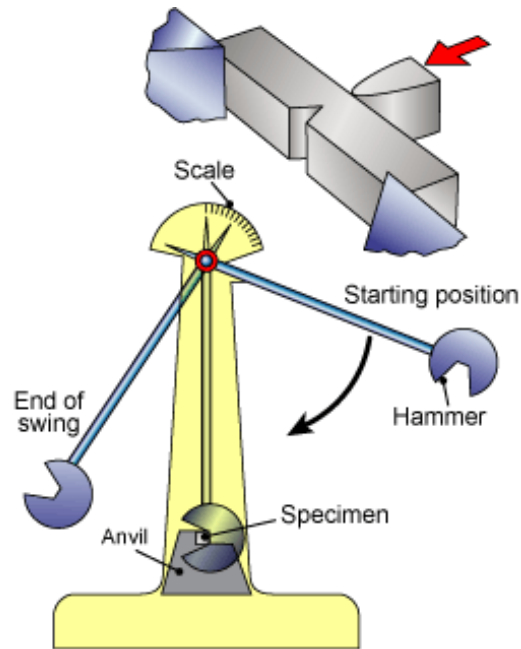


Figure 2.7 Charpy Impact Test

2.3.4 Wear Mechanism

Wear is the progressive loss of materials from contacting surfaces relative in motion. Along with fatigue and corrosion, wear has been known as one of the three major factors limiting the life and performance of an engineering component and an engineering system, whether the system is as big as a heavy machine, or as small as a tiny electronic device [36].

Wear processes can be classified into different types according to the type of tribological load and the materials involved, e.g., sliding wear, fretting wear, abrasive wear, and material cavitation. Wear is caused by a number of mechanisms, the following four being especially important [37]:

1. Surface fatigue is the wear that occurs as result of the formation and growth of cracks. It means Fatigue wear occurs when surface and subsurface cyclic shear

stresses or strains in the softer materials of an articulation exceed the fatigue limit for that material.

2. Abrasive wear is the wear produced by a hard, sharp surface sliding against a softer one and digging out a groove. It means abrasive wear occurs between surfaces of the different relative hardness. In an abrasive wear mechanism, micro roughened regions and very small asperities on the harder surface locally plow through the softer surface.

3. Adhesive Wear is the only universal form of wear and many sliding systems it is also the most important. It arises from the fact that during sliding regions of the adhesive bonding called junctions form between the sliding surface. If one of these junctions does not break along its original interface then a chunk from one of this sliding surface will have been transferred to the other surface. It means Adhesive wear occurs when the atomic force occurring between the materials in two surfaces under relative load are stronger than the inherent material properties of either surface.

4. Corrosive Wear is in a corrosive environment and the sliding action continually removes the protective corrosion product. Corrosive wear can be considered as an accelerating mechanism for corrosion itself, because the motion of an articulation can remove corrosive products and the protective passive layer sooner than interfaces with no relative motion [38].

The specific wear rate (W_s) of the specimen is calculated in the following [39]

$$W_s = \frac{\Delta V}{S_s \times F_N} \quad (2.11)$$

Where S_s = Sliding distance (cm), F_N = Normal load (N)

One guiding principle used in the selection of wear-resistant materials is that high hardness means good wear resistance. Wear resistant hard materials are generally of greater hardness than heat-treated steel and are often consisting of low fracture toughness. Where possible, abrasion, erosion, and wear-resistance data will be provided

concerning the materials listed. The data will be from standard ASTM tests such as the rubber wheel abrasion test, block-on-ring, pin-on-disk [40] and air jet erosion tests. In addition to wear properties, mechanical, physical and thermal properties will be provided. When dry sliding friction creates sufficient surface heating, especially at localized spots, a rapid rise and fall of temperature will produce spalling and an acceleration of wear [41]. Nadendla Srinivasababu found that the wear of the material is not only influenced by the speed of testing but also with load and testing time [42].

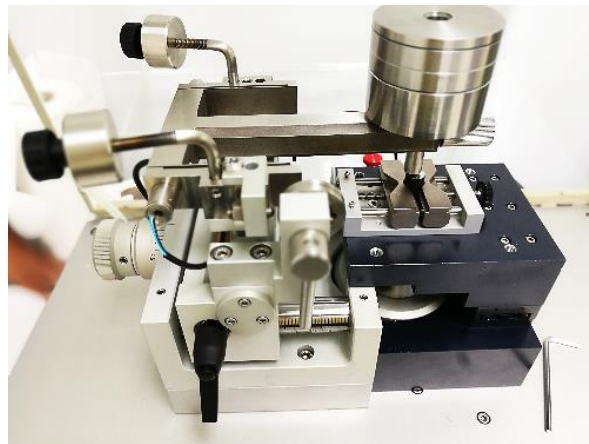


Figure 2.8 Wear Test

2.4. Sheet Metal Forming

Sheet metal forming is one of the most widely used manufacturing processes for the fabrication of a wide range of products in many industries. In present day industry, where the costs play a very important role, the sheet metal products have replaced many products made by forming process [43]. The reason behind sheet metal forming gaining a lot of attention in modern technology is due to the ease with which metal may be formed into useful shapes by plastic deformation processes in which the volume and mass of the metal are conserved and the metal is displaced from one location to another [44].

2.4.1 V-Die Bending

V-Die Bending is widely used throughout industry because of its simple tooling. During V-die bending, the punch moves down, coming first to contact with the unsupported sheet metal. By progressing farther down, it forces the material to follow along, until bottoming on V shape of the die at the final stage [45].

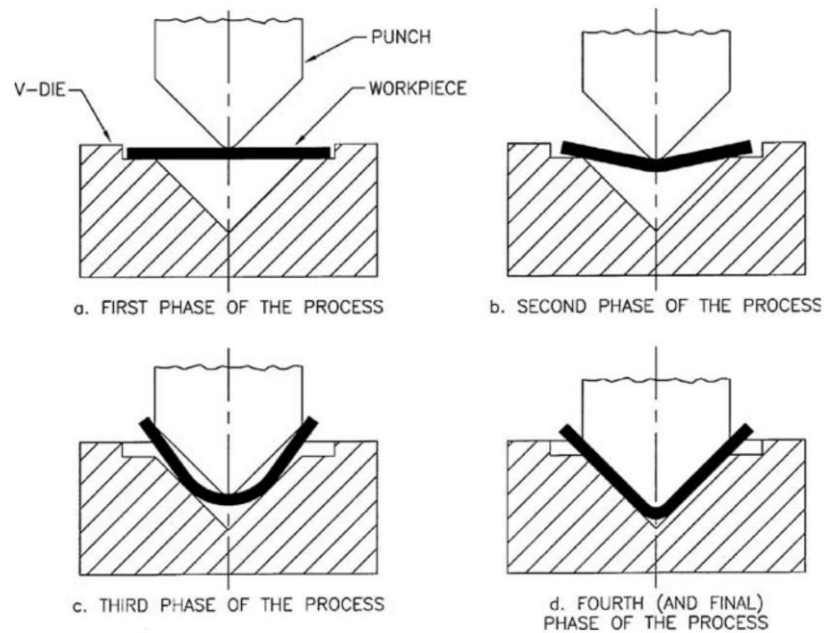


Figure 2.9 V-Die Bending: description of a process

2.4.2 Stress Concentration

Stress Concentration is defined as - Localized stress considerably higher than average (even in uniformly loaded cross sections of uniform thickness) due to abrupt changes in geometry or localized loading [46].

Geometric discontinuities cause localized stress increases above the average. A stress raiser's effect can be determined quantitatively in several ways, but not always readily. The simplest method, if applicable, is to use a known theoretical stress concentration factor, K_t , to calculate the peak stress from the nominal, or average, value;

$$\sigma_{\max} = K_t \sigma_{\text{avg}} \quad (2.12)$$

Stress Concentration factors are obtained analytically from the elasticity theory, computationally from the finite element method, and experimentally using methods such as photo elasticity or strain gages [47].

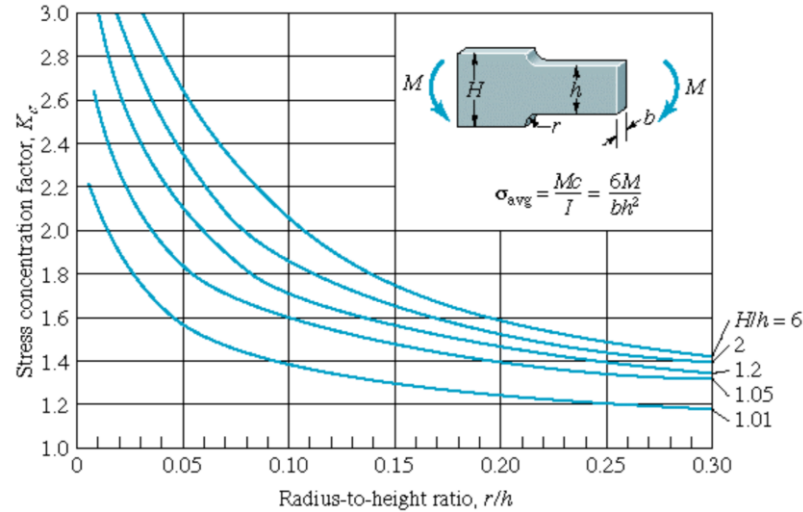


Figure 2.10 Stress Concentration Factor for Rectangular Plate with Fillet (Bending Load)

2.4.3 Application in FEM

The finite element method (FEM) is a numerical procedure that can be used to obtain solutions to a large variety of engineering problems such as structural, thermal, heat transfer, electromagnetism and fluid flow [48]. FEM is a good choice for the analysis of sheet metal processes. The FEM simulations are increasingly used for investigating and optimizing the processes [49].

2.4.4 Computer Simulation

Computational analysis methods like finite element analysis (FEA) have progressed from validation and failure verification tools to design and concept verification tools, resulting in them being employed earlier in design cycles where analysis results drive the design process [50].

Hooke's Law is the linear relationship between stress and strain for a bar in simple tension or compression. It is expressed by the Equation 2.13.

$$\sigma = E\delta \quad (2.13)$$

σ is the axial stress, δ is the axial strain, and E is a constant of proportionality known as the modulus of elasticity for the material. The modulus of elasticity is the slope of the stress-strain diagram in the linearly elastic region. Since strain is dimensionless, the units of E are the same as the units of stress. Typical units of E are psi or ksi in USCS units and pascals (or multiples thereof) in SI units [34].

Material non-linearity results from the non-linear relationship between stresses and strains. There exist various models, which define non-linear material behavior. Elasto-plastic, Elasto-viscoplastic, and creep nonlinear behaviors are some examples for material non-linearity [45].

The Von Mises Criterion is the most widely used one because of its success due to the continuous nature of the function that defines this criterion and its agreement with the observed behavior for the commonly confronted ductile materials [51]. The Von Mises Criterion states yielding occurs when the effective stress (equivalent) equals the yield stress (σ_y) as measured in a uniaxial test. The Von Mises yield criterion for any stress condition is [52]:

$$(\sigma_{xx} - \sigma_{yy})^2 + (\sigma_{yy} - \sigma_{zz})^2 + (\sigma_{zz} - \sigma_{xx})^2 + 6(\tau_{xy}^2 + \tau_{yz}^2 + \tau_{zx}^2) = 2\sigma^2 \quad (2.14)$$

Where σ 's and τ 's are normal and shear stresses, respectively, or

$$(\sigma_1 - \sigma_2)^2 + (\sigma_2 - \sigma_3)^2 + (\sigma_3 - \sigma_1)^2 = 2\sigma^2 \quad (2.15)$$

In terms of principal stresses σ_1 , σ_2 , and σ_3 .

2.4.5 Residual stress

Residual stresses play an important role in the performance of machined components and structures, namely, in the following aspects fatigue life, corrosion resistance and part distortion. It is commonly found that the absolute value of the residual stress close to the surface of the workpiece is high and decreases as the depth

increases. Residual stress can be tensile or compressive and the stressed layer can have multiple depths, depending upon the cutting conditions, working material, cutting tool geometry and contact conditions at the tool/chip and tool/workpiece interfaces. Compressive residual stresses generally improve component performance and life because they promote a tensile stress and prevent crack nucleation. On the other hand, tensile residual stresses tend to increase stresses which lead to premature failure of components. These residual stresses may affect dramatically the performance of the machined part causing its premature failure, excessive wear and corrosion [53].

2.4.6 Corrosion

SCC failures. The term "Stress-Corrosion Cracking" is usually used to describe failures in metallic alloys. However, other classes of materials also exhibit delayed failure by environmentally induced crack propagation. The stresses required to cause SCC are small, usually below the macroscopic yield stress, and are tensile in nature. The stresses can occur from applied external load, but residual stresses often cause SCC failures [54]. Stress Corrosion Cracking is a form of cracking due to a process involving conjoint corrosion and straining of a metal due to residual or applied stresses [55].

Chapter 3 Experimental Procedure

3.1. Heat Treatment Process

3.1.1 Material

Carbon steel is the most prevalent type of steel which can provide material properties that are acceptable for many applications. The JIS SNCM 439 steel is used commercially as a high-strength steel. It is a material that combines high hardenability with high ductility, high wear resistance, good toughness, and good weld ability. It has high fatigue resistance, when properly hardened and tempered [56]. The raw materials used to produce the pin part and the test specimen in this study is JIS SNCM 439. Figure 3.1 shows the size of a test specimen. Chemical composition of the test specimens is shown in Table 3.1.

Table 3.1 Chemical Composition

C (%)	Si (%)	Cr (%)	Ni (%)	Mn (%)	Mo (%)	P (%)	S (%)
0.36-	0.15-	0.60-	1.60-	0.60-	0.15-	≤0.030	≤0.030
0.43	0.35	1.00	2.00	0.90	0.30		

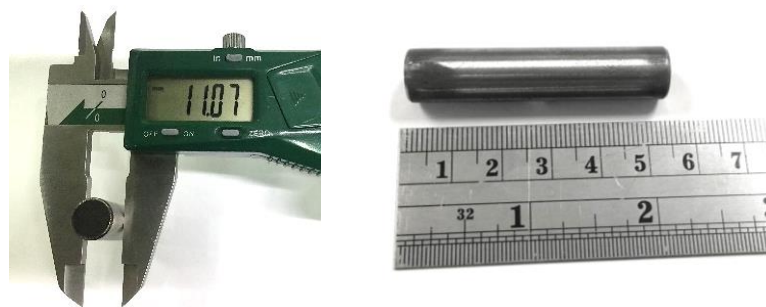


Figure 3.1 Dimension of Specimen

3.1.2 Furnace

The heat treatment furnaces of the factory are rotary retort furnaces which have the capacity of a 60 kg/batch, as shown in Figure 3.2. The specimens can be charged from the front door of the furnace. The furnace is continuously rotated during the process to let the heat transfer throughout the specimens evenly.



Figure 3.2 Rotary Retort Furnace

3.1.3 Hardening Agent

The charcoal is made from Asiatisk Mangrove (Mai Gong Gang) and was crushed into powder as shown in Figure 3.3. The charcoal used in the heat treatment process was brought from two different suppliers: Charcoal No.1(CA) was used in the heat treatment process of the original products and the experiment specimens whereas, Charcoal No.2 (CB) was used in the heat treatment process of the experiment specimens only. In this experiment, the hardening agent in the heat treatment process of the experiments is made from charcoal, with barium carbonate mixed together as shown in Table 3.2. As described in [57], the barium carbonate used in the mixture should not exceed 20 Wt%. to ensure reaction efficiency. The experiments and the heat treatment process of the factory use the same type of charcoal. However, some mixtures of hardening agent used in the experiment differentiate from that used in the heat treatment process of the original product by adjusting ratio of barium carbonate (BaCO_3). From the study it was found that urea can improve mechanical properties Therefore, in order

to improve the surface hardness of the specimens, 10% of urea was added to the CB mixture (CN) as shown in Table 3.2.



Figure 3.3 Charcoal Powder to be used as a Hardening Agent

Table 3.2 Hardening Agents in the Experiments

Hardening Agents	Mixtures of Hardening Agent	Ratio of Mixture
CA	Charcoal: Barium carbonate	80:20
CB	Charcoal: Barium carbonate	85:15
CN*	Charcoal: Barium carbonate: Urea	75:15:10

*CN mixture was not analyzed by PROXIMATE ANALYSIS OF COAL

The mixtures of hardening agent were analyzed by PROXIMATE ANALYSIS OF COAL under ASTM D1762-84 [58]. The results from the test of hardening agents demonstrate volatile matter, fixed carbon and ash. The mixtures used in the original production process have an 80/20 (CA) blend ratio of charcoal: Barium carbonate (BaCO_3), in this experiment, the new mixtures with 85/15 ratio (CB) were also used for testing. The new mixtures (CB) have a higher content of fixed-carbon and a lower ash content, which shows that this might be preferable for the hardening process as opposed to the original hardening agent as shown in Table 3.3.

Table 3.3 Results from Analyzed Hardening Agent

Parameters	Charcoal (No.1): CA	Charcoal (No.2): CB
Moisture content (%)	2.86	6.66
Volatile matter (%)	18.93	36.73
Ash (%)	56.25	31.25
Fixed carbon (%)	21.96	25.36

3.1.4 Heat Treatment

The original temperature that the factory used in the heat treatment process was lower than A_3 in Iron-Carbon Phase Diagram (Figure 3.4) which cannot effectively improve the mechanical properties of the specimens. Therefore, in this research the temperature was increased to 830 °C as it is a recommended temperature for austenitizing carbon and low-alloy steels prior to hardening for the specimens [59].

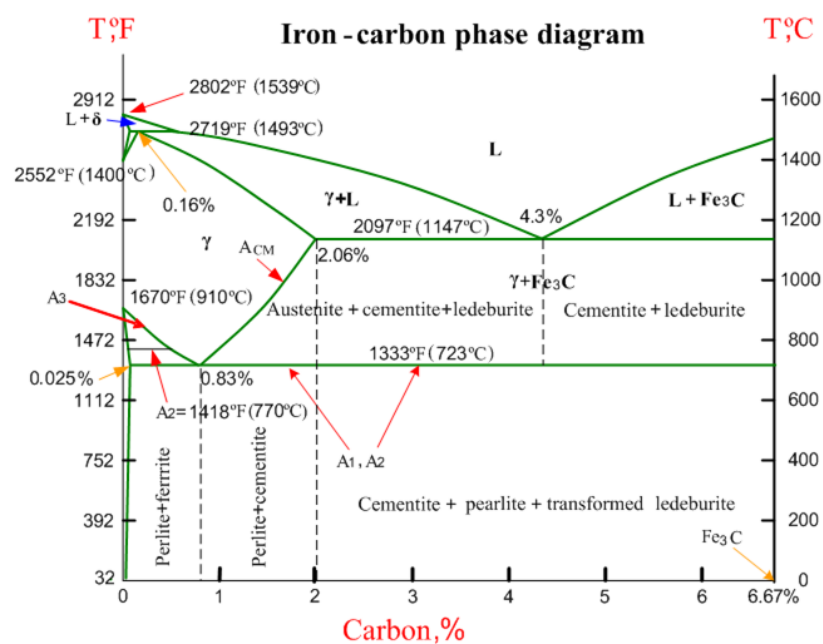
**Figure 3.4 Iron-carbon phase diagram [60]**

Figure 3.5 presents the original heat treatment process of the factory and the heat treatment process of the experiments. In the original heat treatment process, the specimens and the charcoal-BaCO₃-mixture are charged into the furnace (A) with a temperature of 800 °C. After the temperature dropped and was raised up to 830 °C, the holding period begins. At 830 °C the austenitizing occurs [61]. The holding period time depends on the size of specimen. After that, the specimens are quenched by oil.

The heat treatment process of the experiments is similar to the original process. In the experiments, the same furnace is used to run the tests. However, the hardening agents are charged at different time of the holding periods: the beginning of the holding period (B) and the mid-point of the holding period (C). After quenching, all specimens are tempered at 200-230 °C for 30 minutes. The temperature used for tempering process are controlled to be lower than 300 °C in order to avoid tempered embrittlement [62].

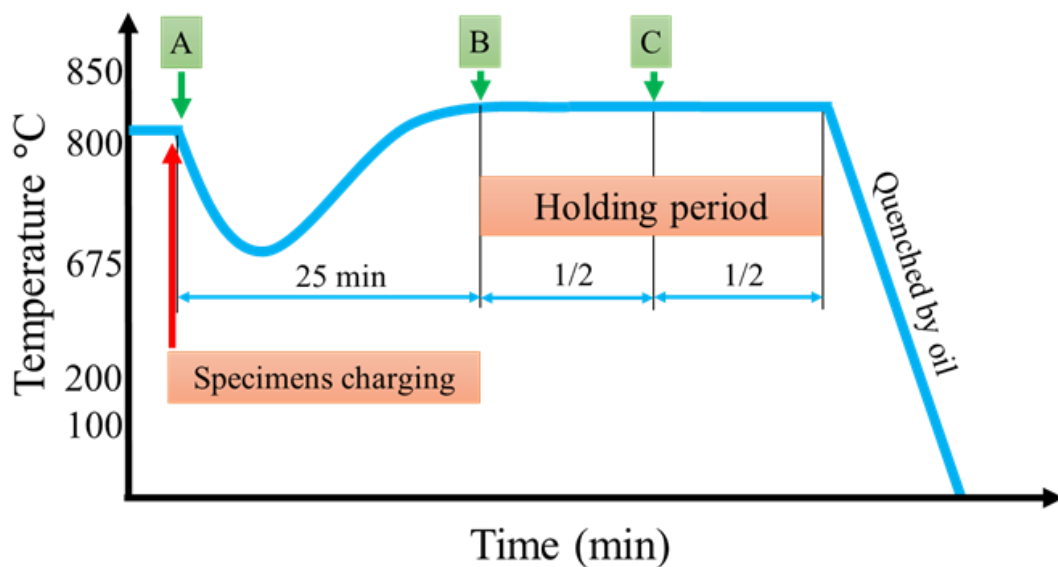


Figure 3.5 The Heat Treatment Process

The specimens used in this experiment are parts of the pin diameter, with dimension of 11mm, 9.5 mm and 5.9mm, which is shown in Table 3.4 and represents the amount of hardening agent and the holding period used in each of the experiments.

The 11 mm Pin diameter was tested by the addition of the hardening agent together with the specimen into the furnace, then an additional dosage of hardening

agent at the mid-point of the holding period. In the experiments, the different mixtures of charcoal+BaCO₃ with and without adding the urea were charged during the heat treatment process as a hardening agent to elicit carburizing and carbonitriding reactions at the surface of the specimens.

The experiment design of the 9.5 mm pin was conducted after considering the results from the 11 mm pin, using the same ratio of mixtures with different amounts of hardening agent and charging at different periods. The specimens are smaller than the 11 mm pin; therefore, the hardening agent when added at the mid-point of the holding period in the heat treatment process should not exceed 150 grams. In order to study the difference of mechanical properties, the additional charging of the hardening agent was tested as follows: 1. CB-30 is the addition of hardening agent without urea with specimens into the furnace and incorporating the hardening agent at the mid-point of the holding period; 2. CN-30s is the addition of hardening agent (mixture of urea) with specimens into the furnace; and 3. CN-30h is the addition of hardening agent (mixture of urea) with specimen into the furnace and incorporating the hardening agent at the beginning of the holding period.

The mechanical properties of the 11 mm and 9.5 mm pin parts were analyzed to design the heat treatment process for improving the mechanical properties of 5.9 mm pin parts. The experiment was carried out by adjusting the amount of hardening agent charged into the furnace with the specimens and the constant amount of the hardening agent charged into the furnace at the mid-point of the holding period.

Table 3.4 The Test Conditions of the Experiment

No.	Test conditions	Time point of Hardening agent Charged (see Figure 3.4)			Note
		A	B	C	
1	Original product	20 g			Pin 120G (11 mm), 100G (9.5 mm), 2060 (5.9 mm)
2	CA-01	20 g		100 g	Pin 120G ϕ 11 mm
3	CA-02	20 g		120 g	
4	CB-01	20 g		120 g	
5	CB-02	20 g		150 g	
6	CN-01	20 g		100 g	
7	CN-02	20 g		50 g	
8	CB-30	20 g		30 g	
9	CN30-S	30 g			
10	CN-30h	20 g	30 g		
11	CN-20-30	20 g		30 g	Pin 2060 ϕ 5.9 mm
12	CN-30-30	30 g		30 g	
13	CN-40-30	40 g		30 g	

3.2. Characterizations

3.2.1 Hardness Test

1. Rockwell Hardness

Rockwell Hardness Test was used to control the quality of parts from the factory. The surface of the specimen was prepared by polishing. Then the specimens were measured by the Rockwell (Scale A) hardness for 3 positions as shown in Figure 3.6.

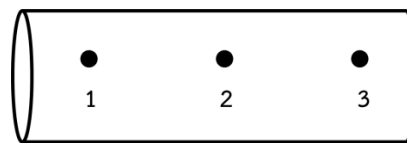


Figure 3.6 Measurement Position of Specimen

2. Micro Vickers Hardness

The comparison between the hardness of test specimens and the original products were carried out by measuring the Vickers hardness along the cross-section diameter of the specimens for 13 points plus 2 more points at the edge as shown in Figure 3.7 (A). The picture of the Vickers hardness test points on the specimen is shown in Figure 3.7 (B). Its purpose is to investigate the improvement of hardness profile near the surface which is related to the wear resistance [63]. The applied test load used in this test was 500-gram force (gf), which is generally used for this material [64].

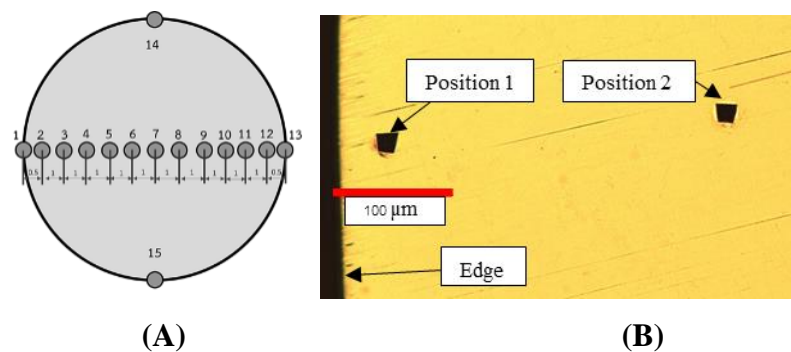


Figure 3.7 Vickers Hardness Test (A) Measurement Positions, (B) Points on The Specimen

3.2.2 Charpy Impact Test

The Charpy Impact Test investigates the toughness of specimen after the heat treatment process as shown in Figure 3.8. The impact test uses the internal unit to analyze under specification of factory which is not less than 122 TMI scale A (a measurement unit set up and used by the factory) and compares other brands. In the test, the hardness is measured first and then the impact tested after.



Figure 3.8 Charpy Impact Test Machine

3.2.3 Dry Sliding Wear Test

The pin-on-disk wear test has been conducted. The tribology testing machine is shown in Figure 3.9 (A). During the test, the top surface of the test specimens was reciprocated by a tungsten carbide ball. Afterwards, the wear profiles of the specimens were measured by using the profilometer. The degree of wear is analyzed by using the wear loss area of zone-B1 [65] as shown in Figure 3.9 (B). The wear loss area was calculated by GeoGebra software. Normally, the wear mechanism of material depends on the relative velocity between the sliding surfaces, temperature, hardness and roughness of the materials [58]. In this study, each wear test has the same test condition as shown in Table 3.5.

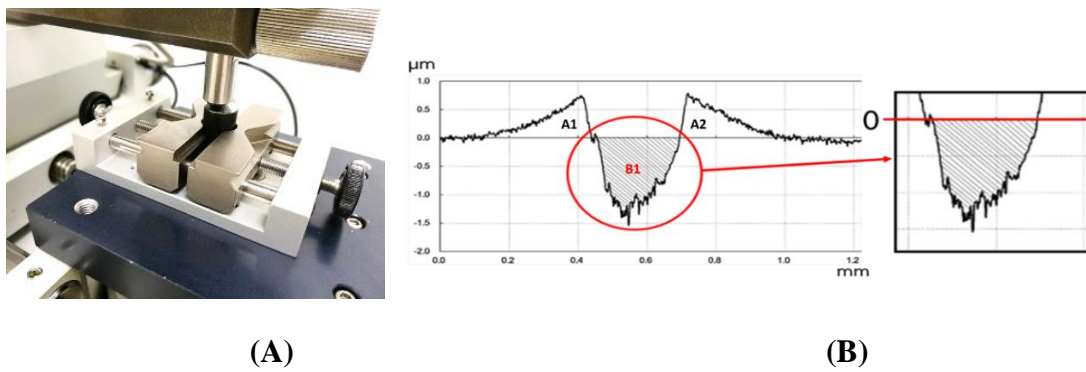


Figure 3.9 Dry Sliding Wear Test (A) Tribology Testing Machine, (B) Cross-section Area Measured by the Profilometer

Table 3.5 Test Condition of Wear Test

Ball	Tungsten carbide
Mode	Linear
Load	10 N
Speed	2 cm/s
Time	15, 30 min

3.2.4 Double Shear Test

During the actual use of the chain, the pin is subject to shearing and bending forces transmitted by the chain link plate. The replica design of the specimen holder equipment for the double shear test is shown in Figure 3.10 (A). The specimen holder consists of 3 metal plates with holes that are the same size as the pin diameter. The tension load is applied to the 3 metal plates. The thickness of the middle plate is the same as the length of roller part in the chain. Toughness results are analyzed by the area under the graph from the double shear test as shown in Figure 3.10 (B).

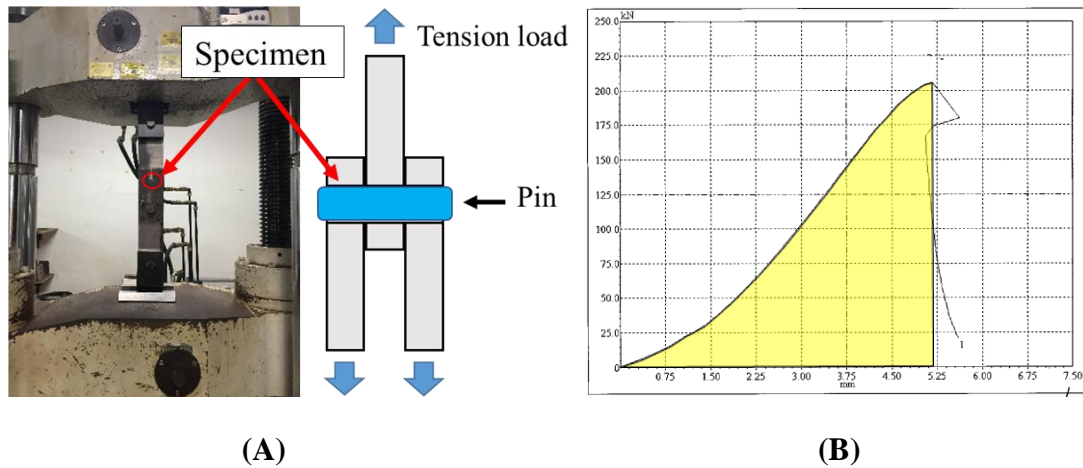


Figure 3.10 Double Shear Test (A) Machine and Specimen Holder Equipment, (B) Double Shear Test Result

3.2.5 Microscopy

The microstructure is analyzed by a Scanning Electron Microscope (SEM) as shown in Figure 3.11 with a test at 1,000 to 3,000x magnification, focusing on the microstructure of the material at the surface of the specimen and the center of the specimen. The EDX technique is used to compare the characteristics of the structure of the material as well as comparing the amount of carbon at the center and the surface of the specimen.



Figure 3.11 Scanning Electron Microscopy

Chapter 4 Results and Discussion

4.1. 11 mm Pin Diameter

The test results of the 11 mm pin through the heat treatment process by the addition of the hardening agent with the specimen into the furnace and the addition of hardening agent at the mid-point of the holding period using different amounts of the hardening agent (see Table 3.4) were analyzed in order to improve surface hardness, wear resistance and to increase the lifetime extension of the roller chain parts. The test results from the different mechanical properties of the specimen are shown as follows:

4.1.1 Internal Results (Measured in the Factory)

The test results pertaining to the mechanical properties of the specimen measured in the factory, by using the Rockwell Hardness Testing and Charpy Impact Testing are shown below in Table 4.1.

Table 4.1 The Internal Results

Mixture Composition of Hardening Agent (Charcoal 80% / BaCO ₃ 20%)					
Code	Hardening Agent (g)	Hardness		Charpy Impact (TMI Scale A)	Note
		HRA	HR15N		
Original product	20	73	81	172	
CA-01	120	75.9	85.6	137	Pass
CA-02	140	75.0	83.9	138	Pass

Mixture Composition of Hardening Agent (Charcoal 85% / BaCO₃ 15%)					
Code	Hardening Agent (g)	Hardness		Charpy Impact (TMI Scale A)	Note
		HRA	HR15N		
CB-01	140	76.4	86.8	117	Pass
CB-02	170	76.3	86.7	103	Fail*
Mixture Composition of Hardening Agent (Charcoal 75% / BaCO₃ 15% / Urea 10%)					
CN-01	120	76.7	87.19	67	Fail*
CN-02	70	75.8	86.7	134.8	Pass
The External Factory Heat Treatment Process					
SN-01	Gas carbonitriding	81.4	89.3	11	Fail*
SN-02	Gas carbonitriding	81.5	89.7	10	Fail*
SN-03	Gas carburizing	79.9	88.0	19	Fail*

* Fail = impact strength is lower than specification

The test results from Table 4.1 show that the hardness of the specimens from the experiments (75-76.7 HRA) is higher than the original product (73 HRA). It can be observed that the amount and the ratio of the hardening agent have a significant effect on the mechanical properties. In addition, the amount and the ratio of the mixture composition of the hardening agent were analyzed to investigate the hardness of the specimens in order to meet with the specification of the factory. The test results revealed that, the hardness and toughness of CA-01 (75.9 HRA, 137 TMI scale A) and CA-02 (75 HRA, 138 TMI scale A) represented almost the same values. As a result, the ratio

and amount of the mixture composition of the hardening agent was relatively adjusted to CB-01 (120 g) and CB-02 (150 g). It was found that the hardness results of the experiment were higher than CA-01 and CA-02. The results show no significant difference between CB-01 (76.4 HRA) and CB-02 (76.3 HRA). However, the toughness of CB-02 (103 TMI scale A) is lower in comparison with CB-01 (117 TMI scale A).

Urea was consequently added to the hardening agent as a new ratio of mixture (CN) and charged during the heat treatment process in order to increase the surface hardness. The results show that the specimen of CN-01 (100 g) reaches the highest value of the Rockwell hardness test (76.7 HRA); however, the result of the toughness (67 TMI scale A) does not meet the specification of the factory. Subsequently, the hardening agent was adjusted to a suitable amount of mixture CN-02 (50 g) and charged during the heat treatment process. As a consequence, the hardness result of CN-02 (75.8 HRA) is lower than the CN-01 and the toughness result of CN-02 (134.8 TMI scale A) is higher than CN-01.

In addition, the specimens were also tested by gas carbonitriding (SN-01 and SN-02) and gas carburizing (SN-03) process. The hardness results of the specimens are remarkably high (79.9-81.5 HRA). However, the toughness of the specimens does not meet the factory specifications requirement. Continuing the tests would be prohibitively expensive due to the process. For this reason, the studies in this section were stopped.

4.1.2 Micro Vickers Hardness Test

In this experiment, Micro Vickers Hardness Test was used to measure the hardness values of the test specimens. The hardness profiles were measured on the cross-sectional diameter of the specimens, see Figure 3.6 (A).

The results are presented in Figure 4. (1-7). The plot graph shows that the Micro Vickers Hardness at the center of the test specimens has the average hardness value of 560 HV, which has no significant difference among each other.

The Figure 4.8 shows the comparison between the hardness at the edge of the specimens (50 microns from the edge) on the cross-sectional surface of the test specimens and the original product. The result shows that the hardness of the experiment specimens is higher than the original product with a hardness value of around 556 HV. The test results revealed that the CN-01 specimen presents the highest hardness value of 615 HV.

One possible reason that causes the lower surface hardness value of the original product compared to the Micro Vickers Hardness at the center of the test specimens can be the occurrence of decarburization during the heat treatment process, which play an important role in decreasing the surface hardness.

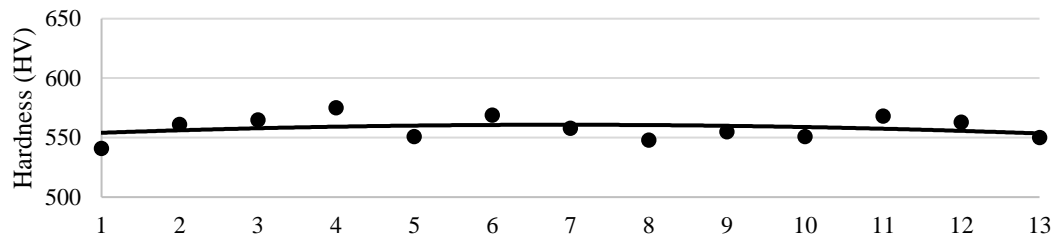


Figure 4.1 Hardness Profile of Original Product

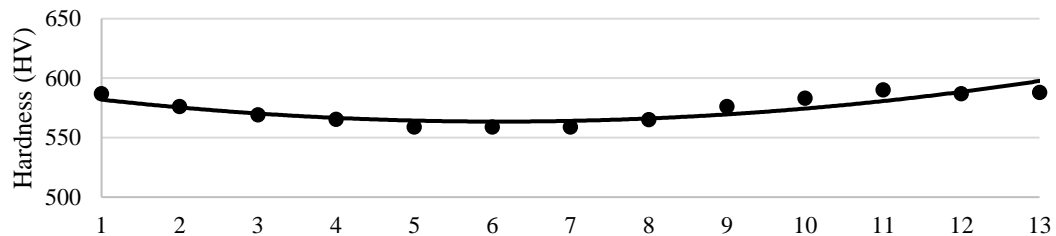


Figure 4.2 Hardness Profile of Experiment CA-01

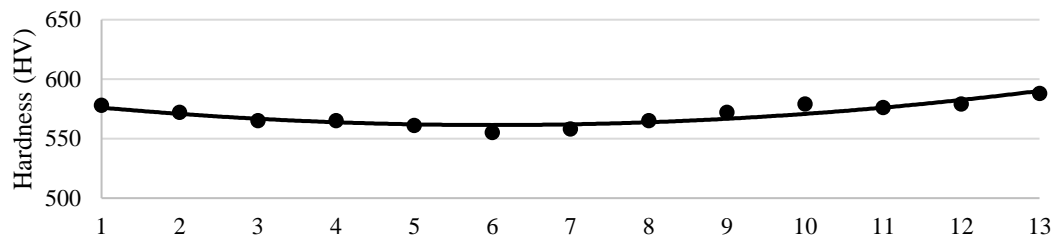


Figure 4.3 Hardness Profile of Experiment CA-02

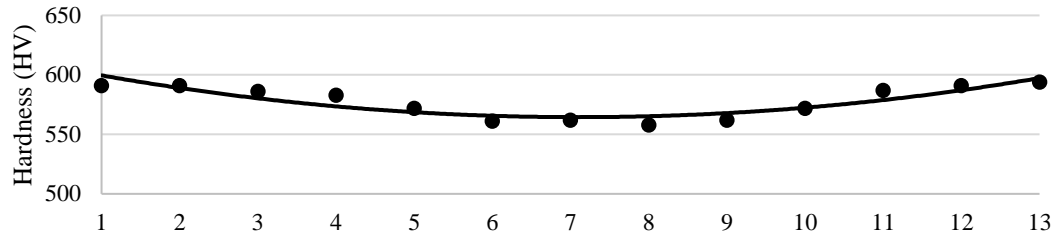


Figure 4.4 Hardness Profile of Experiment CB-01

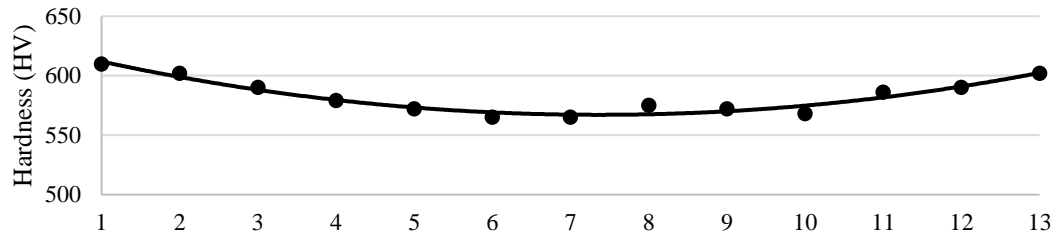


Figure 4.5 Hardness Profile of Experiment CB-02

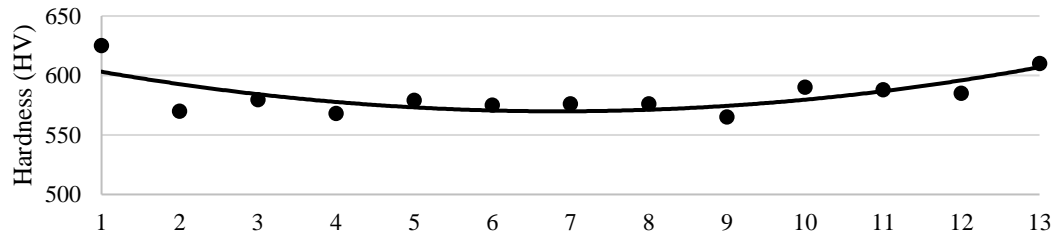


Figure 4.6 Hardness Profile of Experiment CN-01

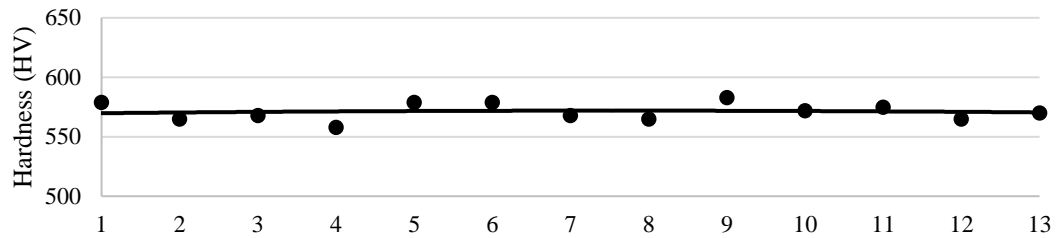


Figure 4.7 Hardness Profile of Experiment CN-02

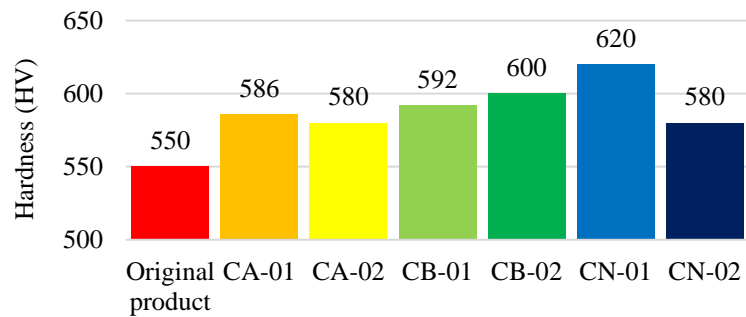


Figure 4.8 Micro Vickers Hardness at the Edge

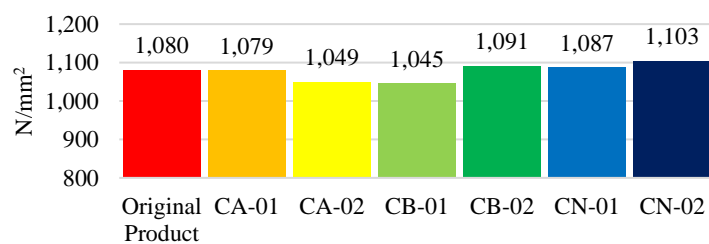
4.1.3 Double Shear Test

The results of shear strength and toughness from double shear tests are shown in Table 4.2, which draws a comparison between the original products and the experiment specimens. The Double Shear Test was measured according to the variability of toughness from the Charpy Impact Test.

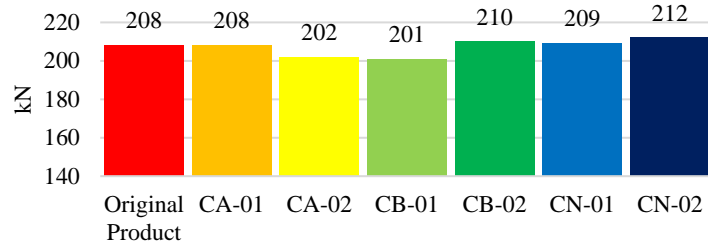
Table 4.2 The Results from Double Shear Test

Code	Shear Strength (N/mm ²)	Maximum Load (kN)	Elongation (mm)	Toughness (J)
Original Product	1,080	208	5.26	478
CA-01	1,079	208	5.89	487
CB-01	1,049	202	5.54	456
CB-02	1,091	210	5.70	440
CN-01	1,087	209	5.32	454
CN-02	1,103	212	5.29	482

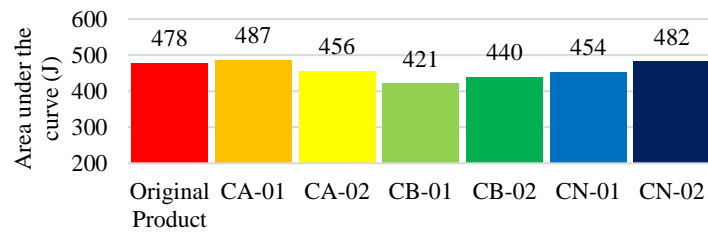
From Figure 4.9 we can see that the results of the Double Shear tests have no significant difference between the original products and the experiment specimens. All results still meet the specification of the factory measured by using the maximum load value, which is not less than 190 kN.



(A)



(B)



(C)

Figure 4.9 The Results from Double Shear Test (A) Shear Strength, (B) Maximum load and (C) Toughness of The 11 mm Diameter

4.1.4 Wear Test

The Wear Test results obtained by measuring the wear loss area from tribology testing machine at the surface of the specimens after 15 and 30 minutes are shown in Table 4.3. The test is a comparison between the original product and the experiment specimens. Figure 4.10 shows the wear loss area of the specimens.

Table 4.3 The Result from Tribology Testing

Code	Wear Loss Area (μm^2)	
	15 min	30 min
Original Product	479	700
CA-01	247	501
CB-01	171	319
CB-02	168	321

CN-01	183	382
CN-02	245	401
E	226	360
S	196	364

The experiment included the addition of the hardening agent into the furnace to improve the wear resistance of the pin part. Initially, the original product showed the highest wear loss area for both cases: after 15 minutes ($479 \mu\text{m}^2$) and 30 minutes ($700 \mu\text{m}^2$). After 15 minutes of the wear test, wear resistance ability of the experiment specimens was approximately 2 times greater than that of the original product. It was found that wear resistance ability from the mixture of the hardening agent CB-02 showed the lowest wear loss area ($168 \mu\text{m}^2$). Followed by the specimens from the mixture CB-01 and CN-01, which has a similar amount of wear loss area ($171 \mu\text{m}^2$ and $183 \mu\text{m}^2$). Whereas the mixture of hardening agent CA-01 and CN-02 provided similar results ($247 \mu\text{m}^2$ and $245 \mu\text{m}^2$), which presented better wear resistance ability in comparison to the original product. After 30 minutes of the wear test, the measured wear loss area of all specimens was increased to nearly double, compared against the test results after 15 minutes.

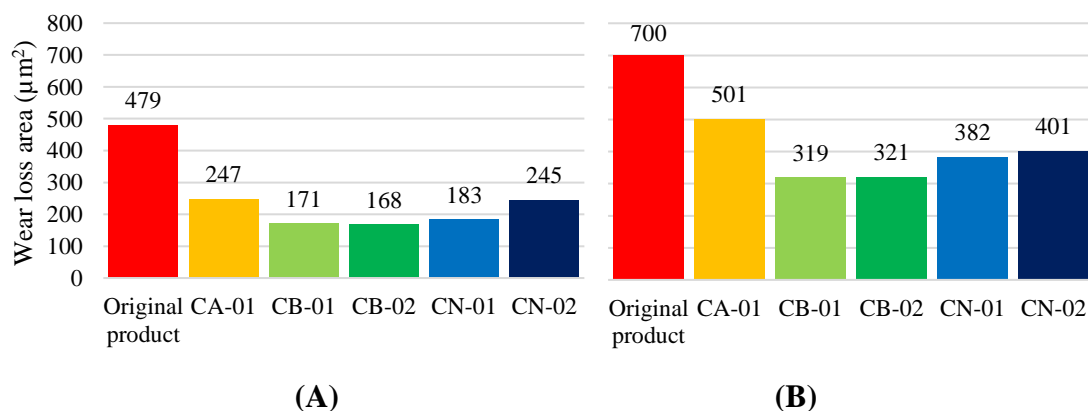


Figure 4.10 Wear Loss Area (A) after 15 minutes, (B) after 30 minutes of The 11 mm Pin Diameter

Figure 4.11 presents the results of the wear loss area between CB-02 and other products. After 15 minutes of the wear test (A) it can be seen that the wear resistance ability of CB-02 represents lower wear loss area ($168 \mu\text{m}^2$) than specimen S ($196 \mu\text{m}^2$) and specimen E ($226 \mu\text{m}^2$). Similarly, the wear test of CB-02 after 30 minutes (B) represents the lowest wear loss area ($321 \mu\text{m}^2$), which provides the best wear resistance ability, compared to specimen E ($360 \mu\text{m}^2$) and specimen S ($364 \mu\text{m}^2$).

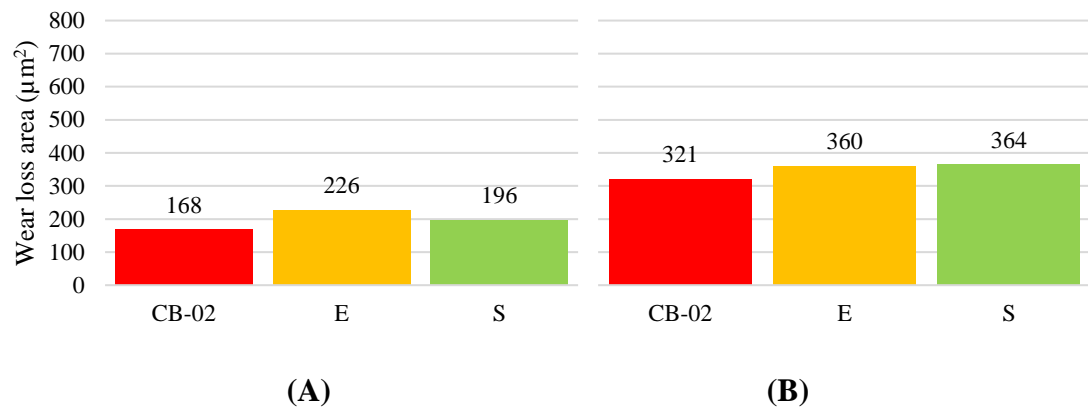


Figure 4.11 Wear Loss Area (A) after 15 minutes, (B) after 30 minutes of The Experiment Specimens and other products

The results can be explained by the fact that the amount and the ratio of hardening agent were suitably adjusted, thereby leading to the prevention of decarburization. Carburizing/Carbonitriding reactions also took place during the heat treatment process, resulting in an increase in the surface hardness of the specimens.

4.1.5 Microstructure

The experiment specimens were investigated after the wear test. The edges of the specimens were analyzed. The SEM micrographs (1,000 - 3,000 magnifications) of the original product and experiment specimens are shown in Figure 4.12-4.14 (A) microstructure at the edge and (B) microstructure at the center of the test specimens respectively.

The micrographs show the microstructure at the edge of the cross-sectional of the specimens. In the case of the original product (Figure 4.12), the microstructure in

the zone of 50-micron decarburization depth mainly consists of retained austenite phase, whereas in the case of the experiment specimens (Figure 4.13-4.14), the microstructure mainly consists of martensite. All the hardened test specimens have similar microstructure to the experiment specimens.

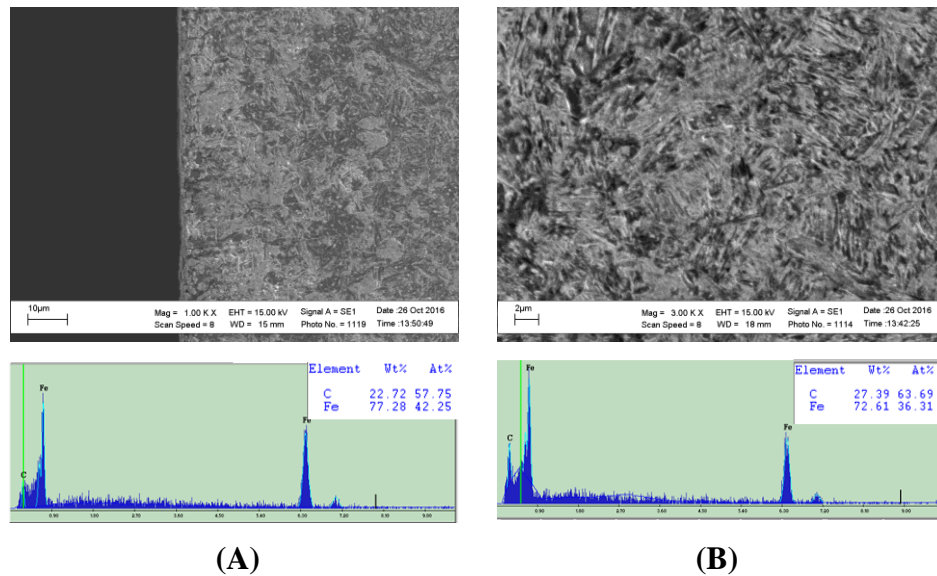


Figure 4.12 Microstructure of The Original Product (A) at the edge and (B) at the center

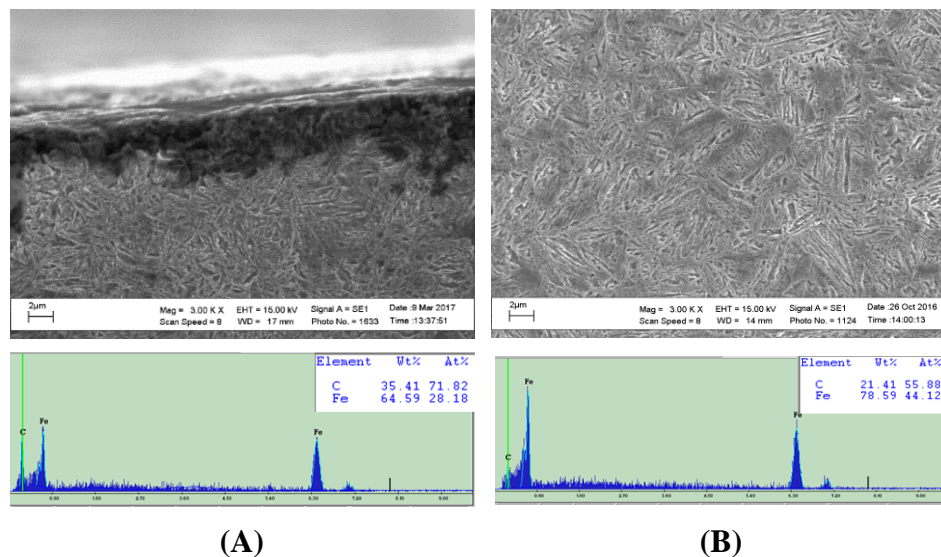


Figure 4.13 Microstructure of the Experiment Specimens in Carburizing Process (code CA, CB) (a) at the Edge and (b) at the Center

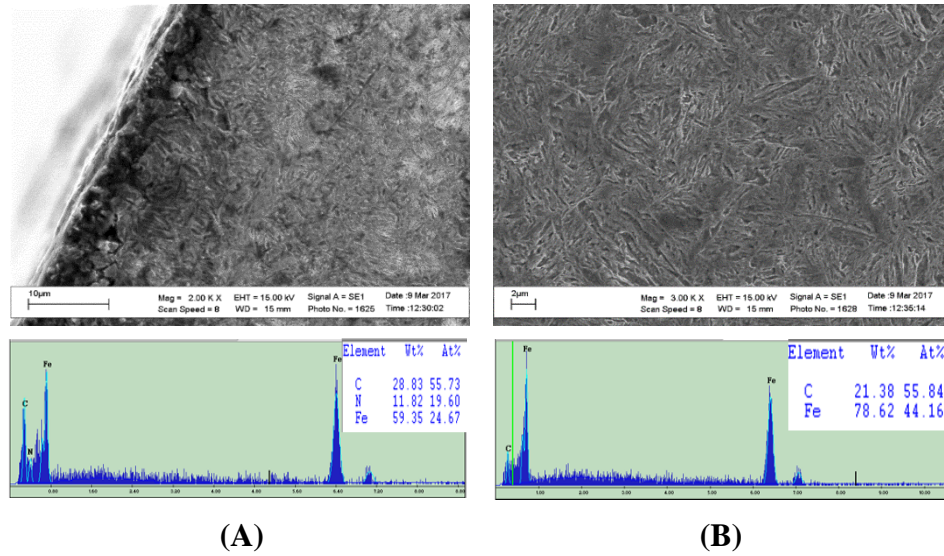


Figure 4.14 Microstructure of the Experiment Specimens in Carbonitriding Process (code CN) (A) at the Edge and (B) at the Center

Table 4.4 The Results from Energy-Dispersive X-ray at the Edges and Center

Specimen	Position	
	Edge (Wt % of carbon)	Center (Wt % of carbon)
Original product	22.72%	27.39%
Without urea (CA, CB)	35.41%	21.41%
Urea Mixture (CN)	28.83%*	21.38%

*11.02 Wt% of nitrogen was found at the edge of the specimen CN

Table 4.4 presents the elemental analysis results from Energy-Dispersive X-ray at the edges and at the center of the original product and the experiment specimens.

The test results revealed that the weight percentage of carbon content in the original product at the edge is 22.72 Wt%. The value at the center of the specimen presents 27.39 Wt%. which shows a higher weight percentage compared to that of the

original product. The results of the experiments can perhaps be explained by the fact that the decarburization still occurs at the edge of the original product. The experiment specimens show 28.83-35.41 Wt% of the carbon content at the edge. It presents a higher weight percentage than the original product as well as providing a better result in wear resistance ability.

Furthermore, 11.02 %Wt of Nitrogen was found at the edge of the specimen CN. One possible reason can be the hardening agent mixture of urea, which plays an important role in increasing the surface hardness of the specimens.

4.1.6 Discussion

The results of the experiment from the addition of the hardening agent into the furnace to improve the wear resistance of the pin part showed that the amount and the ratio of the hardening agent used have a significant effect on the mechanical properties. The suitable amount of the hardening agent used has a significant influence on the surface hardness of the specimens. Excessive amounts of the hardening agent can cause embrittlement and excessive hardness values of the specimen that do not meet the factory specification requirements.

The results of the tests within the factory cannot identify the wear resistance due to and insufficient testing machine. Moreover, the impact test results from the factory are varied. The results cannot be used to analyzed against to the double shear test results which are more reliable. It was found that the results of the shear strength and toughness from the double shear tests have no significant difference between the original products and the experiment specimens. In addition, the hardness results obtained from the micro Vickers hardness test correlate positively with the results of the wear test.

The results of the 11 mm pin from the experiment indicated that the CB-02 specimen showed the best wear resistance. However, the highest amount of hardening agent was added into the furnace (150 g). The second highest wear resistance was shown to be CN-01, which is slightly less than the CB-02 by adding a lesser amount of

the hardening agent (100 g) in the experiment. The experiment showed that the wear resistance ability of both CB-02 and CN-01 had improved approximately 50% or double compared to that of the original product.

4.2. 9.5 mm Pin Diameter

The experiment design of the 9.5 mm pin was conducted after considering the results from the 11 mm pin, using the same ratio of mixtures with different amount of hardening agent and was charged at different periods, see Table 3.4 and Figure 3.4. The test results of the different mechanical properties of the specimen are shown as follows:

4.2.1 Internal Results

The test results of the mechanical properties of the specimens obtained by using similar measurement as the experiment of the 11 mm pin. The hardness test and impact test results were tested from the factory as shown in Table 4.5.

Table 4.5 The internal results

Code	Hardening Agent (g)	Hardness		Charpy Impact (TMI Scale A)	Note
		HRA	HR15N		
Original product	20	73	82	126	-
CB-30	50	75.8	85.3	78	Pass
CN-30s	30	75.5	85.2	79	Pass
CN-30h	50	74.8	84.3	79	Pass

The test results from Table 4.5 show that the hardness of the experiment specimens (74.8-76 HRA) is higher than the original product (73 HRA). In the experiments, the CB-30 presents the highest hardness value of 75.8 HRA. Followed by the specimens from the mixture CN-30s (75.5 HRA). Both results represent almost the

same hardness values. From the table we can see that CN-30h shows the lowest hardness value of 74.8 HRA.

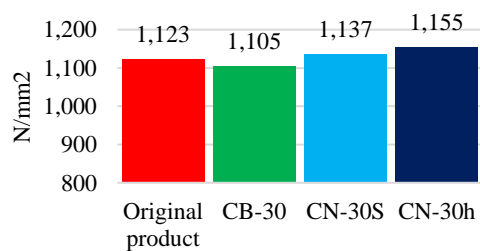
4.2.2 Double Shear Test

The results of shear strength and toughness from the double shear tests are shown in Table 4.6. In comparison with the test results, there is no significant difference between the original products and the experiment specimens.

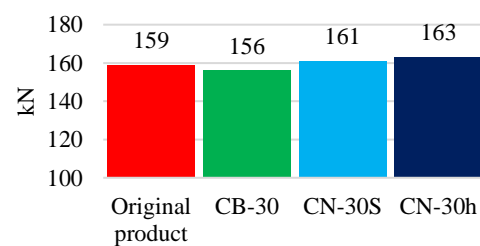
Table 4.6 The Results from Double Shear Test

Double Shear Test	Shear Strength (N/mm ²)	Maximum Load (kN)	Elongation (mm)	Toughness (J)
Original product	1,123	159	4.74	283
CB-30	1,105	156	4.53	267
CN30-S	1,137	161	4.61	300
CN-30h	1,155	163	4.28	282

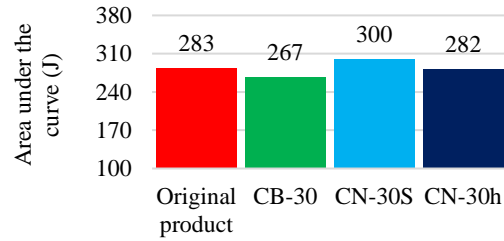
Figure 4.15 (A) shows the results from the double shear test. It can be seen that the results show no significant difference among each other. Figure 4.15 (B) shows the maximum load results. It presents almost the same values. All results still meet the specification of the factory which is not less than 120 kN. Figure 4.15 (C) presents area under the curve or toughness.



(A)



(B)



(C)

Figure 4.15 The Results from Double Shear Test (A) Shear Strength, (B) Maximum Load, and (C) Toughness of The 9.5 mm Pin Diameter

4.2.3 Wear Test

The wear test results were highlighted in Table 4.7. The 9.5 mm pin was examined under the same conditions as the 11 mm pin. The test results revealed that the CB-30 specimen showed the best wear resistance.

Table 4.7 The Results from Tribology Test

Code	Wear Loss Area (μm^2)	
	15 min	30 min
Original product	619	740
CB-30	368	415
CN-30s	541	731

In the experiment, the hardening agent was added into the furnace to improve the wear resistance of the pin part. Initially, the original product showed the highest wear loss area for both cases: after 15 min ($619 \mu\text{m}^2$) and 30 min ($740 \mu\text{m}^2$).

These results indicate that the wear resistance ability from the mixture of hardening agent CB-30 shows the lowest wear loss area of $368 \mu\text{m}^2$. Followed by the mixture of CN-30s, which presents the wear loss are $541 \mu\text{m}^2$. Both results show better wear resistance ability in comparison to the original product. After 30 minutes of the

wear test, the wear loss area of all test specimens increased higher than that of the test specimens after 15 minutes. However, the experiment specimens provide better wear resistance ability than the original product as shown in Figure 4.16.

From the results of 11 mm pin, it was found that hardness is positively correlated with wear resistance ability. Table 4.5 illustrates that CN-30h has the lowest value of hardness. For these reasons, the specimen was not examined for the wear test.

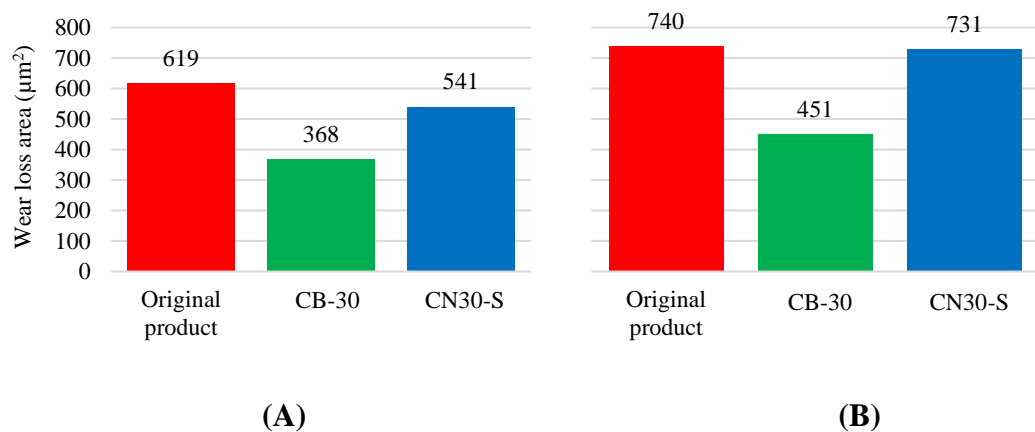


Figure 4.16 Wear Loss Area (A) after 15 minutes, (B) after 30 minutes of The 9.5 mm Pin Diameter

4.2.4 Discussion

The experiment of 9.5 mm pin was carried out from the result of 11 mm pin. The hardening agent was used with the same ratio of mixtures but different amounts of the hardening agent and it was charged at different periods.

The wear test result of CN-30s by the addition of hardening agent (mixture of urea) with the specimen into the furnace indicates that its wear loss area is lower than the original product around 10-15%, which has no significant difference from the original product. Whereas, CB-30 presents the best wear resistance ability, which is 30% higher than that of CN-30s.

The results can perhaps be explained by the fact that the addition of the hardening agent with the specimens at the beginning of the process is not sufficient to improve the wear resistance ability of pin parts. As a result, the hardening agent was

added with the specimens into the furnace and at the mid-point of the holding period to improve wear resistance, thereby leading to an increase in wear resistance ability. This proves that the addition periods of the hardening play an important role increasing the mechanical properties.

4.3. 5.9 mm Pin Diameter

The mechanical properties of the 11 mm and 9.5 mm pin parts were analyzed to design the heat treatment process for improving the mechanical properties of the 5.9 mm pin.

4.3.1 Internal Result

The internal results of the 5.9 mm pin are shown in Table 4.8. The specimens were measured to analyze the mechanical properties.

The test results show the hardness value of the experiments around 74.8-75.0 HRA, which is higher than the original product (73 HRA). All the toughness results from the test specimens meet the specification of the factory.

Table 4.8 The internal results

Code	Hardening Agent (g)	Hardness		Charpy Impact (TMI Scale B)	Note
		HRA	HR15N		
Original product	20	73	82	126	-
CN-20-30	50	74.8	84	102	Pass
CN-30-30	30	75.0	84.3	111	Pass
CN-40-30	70	75.0	85.2	108	Pass

In the experiment, the test results revealed that the hardness and toughness values of CN-30-30 (75.0 HRA, 111 TMI scale B) and CN-40-30 (75.0 HRA, 108 TMI

scale B) represented almost the same values. Finally, the CN-20-30 presents the lowest hardness value from the test (74.8 HRA, 102 TMI scale B).

4.3.2 Wear Test

The experiment results of 5.9 mm pin state that the amount and the addition periods of the hardening agent into the heat treatment process can improve the wear resistance ability.

Table 4.9 highlights the wear test results from tribology testing. The test is a comparison between the original product and the experiment specimens.

Table 4.9 The Results from Tribology Test

Code	Wear Loss Area (μm^2)	
	15 min	30 min
Original product	1,131	1,225
CN-20-30	590	916
CN-30-30	486	967

The Figure 4.17 as shown the wear loss area at 15 minutes and 30 minutes. After the test, the results of the experiment specimens show better wear resistance than the original product. Initially, the original product showed the highest wear loss area for both cases: after 15 minutes ($1,131 \mu\text{m}^2$) and 30 minutes ($1,225 \mu\text{m}^2$). After 15 minutes of the wear test, CN-30-30 shows the best result ($486 \mu\text{m}^2$). After 30 minutes, the test results reveal that there is no significant different between the CN-20-30 ($916 \mu\text{m}^2$) and the CN-30-30 ($967 \mu\text{m}^2$). It was found that the amount of hardening agent effety improved the wear resistance ability of the test specimens.

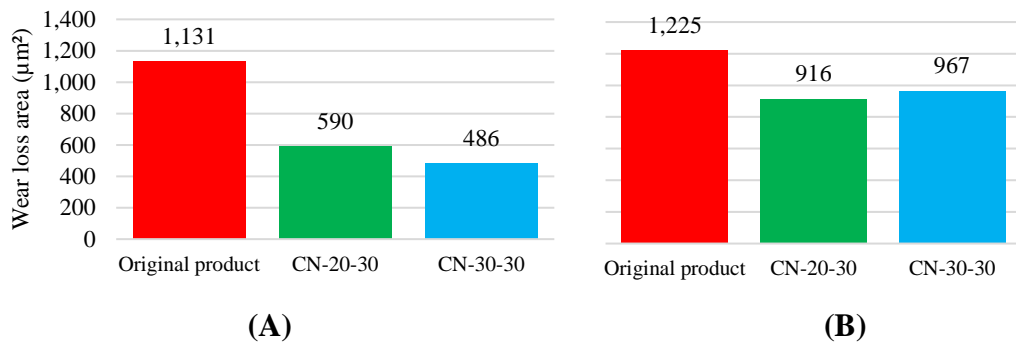


Figure 4.17 Wear Loss Area (A) after 15 minutes, (B) after 30 minutes of The 5.9 mm Pin Diameter

4.3.3 Discussion

An increase in the amount of hardening agent added into the furnace with the specimens can improve the wear resistance ability of the pin part. It can be seen that the wear test results of the test specimen after 15 minutes show better wear resistance than the original product around 50%. However, after 30 minutes, the results of the experiment specimens show almost the same values of the wear loss area whereas, the experiment results present better wear resistance than the original product by around 20%.

This can be due to the insufficient holding period in the heat treatment process; therefore, the addition periods of the hardening agent should be adjusted in order to increase the wear resistance ability of the test specimens.

4.4. Discussion

There are several factors effecting the quality of the roller chain parts in the heat treatment process e.g. the amount of hardening agent, the ratio of mixture, the addition period, the holding period, the duration of the process, and the temperature in the furnace. This research aims to investigate and improve the surface hardness and wear resistance of the roller chain parts, which will result in the chain lifetime extension; therefore, an investigation into the wear resistance ability of pin parts has been conducted in this project.

The test results revealed that the addition of hardening agent with the specimens at the beginning of the process once was not sufficient to improve the wear resistance ability of the pin parts. As a result, the hardening agent was added with the specimens into the furnace and at the mid-point of the holding period, thereby leading to increase in wear resistance ability. The results indicated that this is the best process of improving the wear resistance ability of the pin parts.

The investigation into the mechanical properties of pin parts such as Rockwell hardness test, Charpy impact test and double shear test from the factory cannot indicate the wear resistance ability of the specimens. To find out the wear resistance ability the pin-on-disk wear test has been conducted. It was found that the wear test results obtained from the tribology testing machine are positively correlated with the results of the micro Vickers hardness test.

Furthermore, the results of the experiment showed that the hardening agent without urea showed the best wear resistance. However, the highest amount of hardening agent was added into the furnace. The second highest wear resistance was shown to be the hardening agent with urea, which is slightly less than the hardening agent without urea by adding a lesser amount of the hardening agent in the heat treatment process. This proves that urea plays an important role in increasing the surface hardness of the pin parts.

4.5. Future Work

Heat treatment process is one of the limitations in this study. The timing of the process has an effect on the production of the factory, further research studies need to carry out experiments with different amounts of hardening agents and time points. Furthermore, to characterize carbon diffusion, additional research studies also need to apply other analysis methods such as wear mechanism, numerical analysis and EBSD analysis.

Chapter 5 Computer Simulation

5.1. Background and Problem

The Roller chain is widely used in the transportation industry. In the fish loading process of the seafood industry, the roller chain was used on conveyor belts for carrying fish to the freezer storage. JIS SCM 435 is the carbon steel used to produce the chain plate in the factory. The chain plate was made in the V- die bending and heat treatment process. After that it was used to assemble as components of the roller chain.

Without properly taking care and keeping well maintained by covering the grease, the lifetime of roller chain on the sea fish conveyor belts will usually be shorter than normal due to corrosion from the sea water. After a certain time, stress corrosion cracking might take place during the usage in the loading process and finally lead to the fracture of the chain plate. The fracture in the plate takes place on the bending line at the corner as shown in Figure 5.1. The possible causes of the problem consist of many factors as follows: 1. The raw material used to produce the chain plate is still not most suitable for seawater corrosion (The cost of production is an important factor of the factory; therefore changing materials from carbon steel to stainless steel will increase production costs); 2. The bending line leads to a higher stress concentration at the corner which results in the formation of the cracking during usage; 3. The residual stress caused by the heat treatment process and the tension load during the usage results in the fracture of the chain plate; and 4. Inadequate maintenance of the grease covering during the usage promotes the corrosion rate which lead to the fracture.

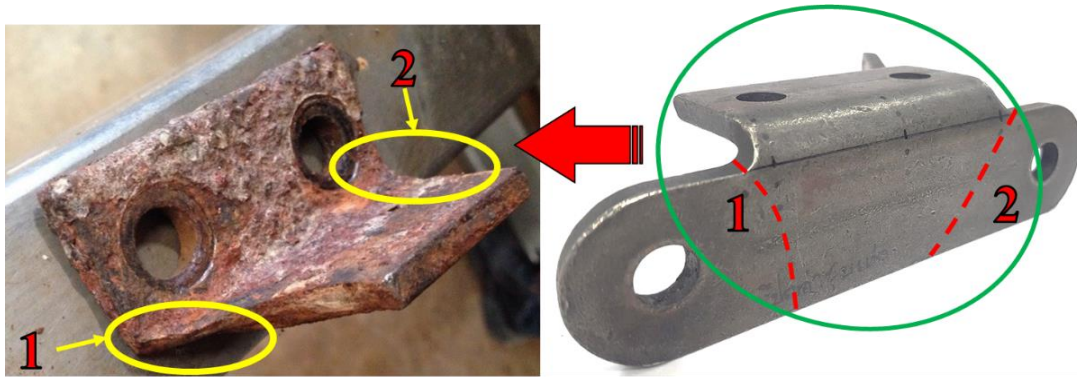


Figure 5.1 Cracking caused Chain Fracture after Usage

The chain manufacturer aimed to increase the lifetime of the chain plate. Under the economical point of view, the factory decided to solve the problem by changing the bending line as it seemed to be the most effective solution without significant effects on the production cost; therefore, only the bending process design was studied in this project.

The cracking of the chain plate during usage and the distribution of stresses on the bending line were analyzed in this part of the study. The computer simulation was used to examine in order to improve the bending process design and to prevent a high stress concentration at the corner which leads to the formation of the cracking. The goal is to extend the lifetime of the chain plate.

In this case, the stress distribution in the bending lines of the chain plate were analyzed by computer simulation software, ANSYS workbench 18.1. Figure 5.2 shows the original bending line (PH-A, 34 mm from the bottom to the bending line), which is located on the fillet zone (between 32 to 36 mm) and the new bending line, which is located above the fillet region, (PH-B, 37 mm from the bottom to the new bending line). The new bending line was examined to reduce the stress concentration. After the bending process, the dimensions of the specimen is still under the standard of the roller chain (ANSI-B29.1). Finally, the results from the computer simulation were validated with the micro Vickers hardness results of the specimens.

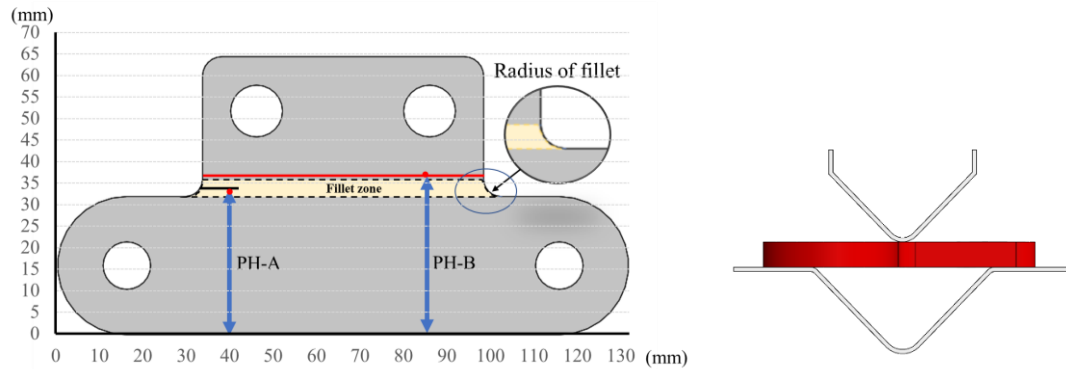


Figure 5.2 Bending line of Chain Plate at 34 mm (PH-A) and 37 mm (PH-B)

5.2. Simulation Setup

Figure 5.3 shows the user interface of ANSYS transient structural program with uploaded CAD model, which was used to analyze the stress concentration of the chain plate. The computer simulation was set up under the conditions stated in Table 5.1-5.4.

The simulation setup outline is on the left size of the program window as shown in Figure 5.3. The simulation setup consists of 4 modules as the following modules:

1. Geometry module, which specifies each part of the specimen,
2. Connections module, which defines the relationship of the components,
3. Mesh module, which defines the accuracy of the simulation response, and
4. Transient structural module, which determines the dynamic response of components of the specimen.

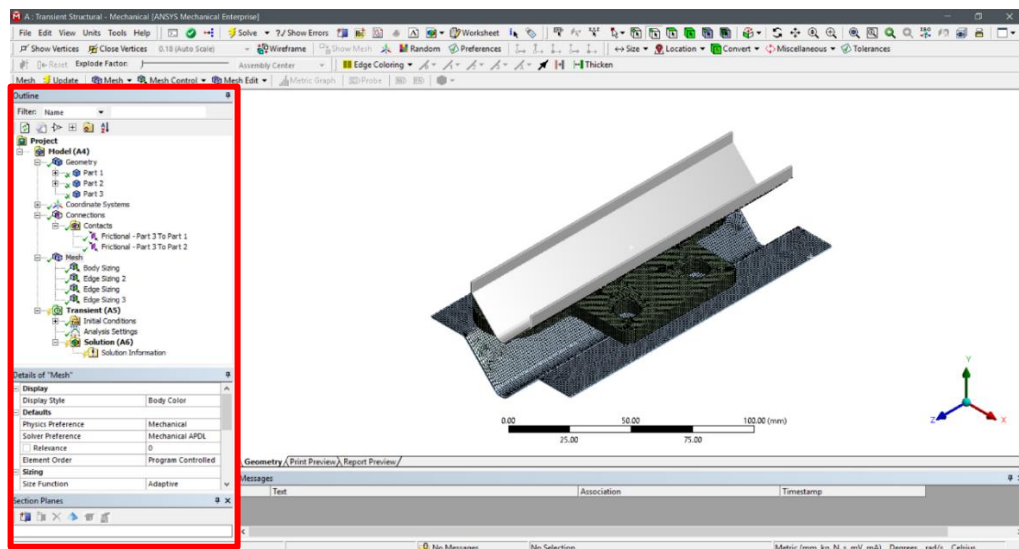


Figure 5.3 Simulation Setup in ANSYS 18.1 Program

5.2.1 Geometry Module

Table 5.1 is the setup conditions for the geometry module. In this simulation, the selected specimen was structural steel. The nonlinear mechanical properties database was used which corresponds to the material properties during the deformation that were transformed from the elastic zone to the plastic zone.

Table 5.1 The Setup in Geometry Module

Geometry Module	
Parts	Stiffness Behavior
Punch	Rigid body
Die	Rigid body
Specimen	Structural steel NL

5.2.2 Connection Module

Table 5.2 shows the connections module setup. Penetration occurs when contact compatibility is disconnect for each part. Therefore, in order to prevent errors, the program must establish a relationship between the both the surfaces. Frictional contact is nonlinear movement; therefore, it was selected in the definition. For frictional contact, friction coefficient must be input. A friction coefficient of 0.1 is used in this case. The Nodal-Normal to Target was set up in the Detection Method as it dictates the direction of forces that are applied at the interface.

Table 5.2 The Setup in Connection Module

Connection Module			
Definition	Detection Method	Contact Bodies	Target Bodies
Frictional	Nodal-Normal to target	Punch, Die	Specimen

5.2.3 Mesh Module

Meshing technique is very important for the setup of the simulation. Meshes produce results with an acceptable level of accuracy. Mesh density is a metric used to control accuracy. It has an effect on simulation results.

Coarse mesh produces results with low accuracy. Although it uses less computational resources and takes a short time to run, it provides a defective solution and cannot be calculated for the solution in some cases. Whereas, fine mesh, a high-density mesh produces results with high accuracy. However, it requires long run times to calculate results. Therefore, the mesh technique should be properly set up for the geometry in the simulation.

Table 5.3 The Setup in Mesh Module

Mesh Module			
Sizing	Mesh Controls		
	Specimen	Punch	Die
Adaptive	Body sizing	Edge sizing	Edge sizing

The mesh module setup is shown in Table 5.3. In this case, the most suitable element size of a specimen is 0.75 mm. The three components have approximately 80,000 elements. Figure 5.4 shows element sizing of the simulation specimens.

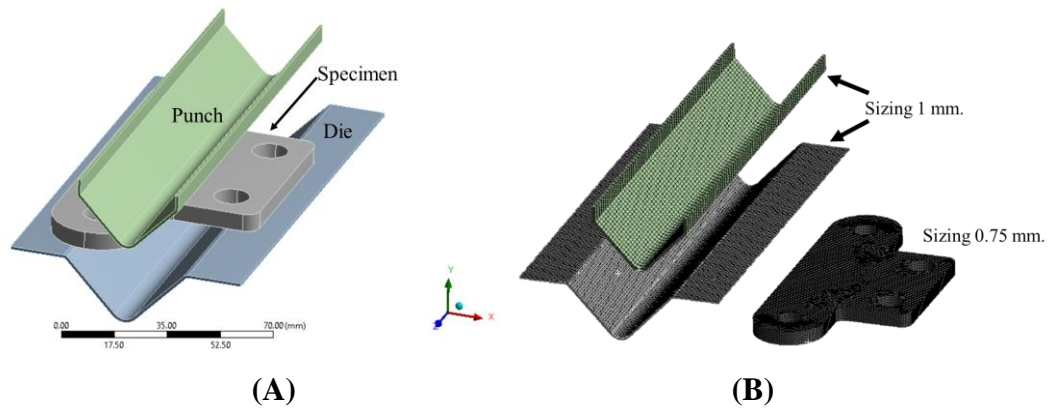


Figure 5.4 (A) Model for Simulation, (B) Sizing of Meshing in Simulation

5.2.4 Initial Conditions Module

Table 5.4 shows the load that is applied by the punch. The velocity of the punch was the same as the factory. The punch takes 2 seconds to move within -Z axis and velocity is at 7.5 mm/s. Finally, after bending the specimen is perpendicular.

Table 5.4 The Setup in Transient Module

Initial Conditions Module			
Geometry	Velocity		
	X	Y	Z
Punch	0 mm/s	0 mm/s	-7.5 mm/s
Analysis Setting Module			
Number of Steps		Step End Time	
1		2 s	

5.3. Simulation Results

Figure 5.5. shows the simulation results of the chain plate on the original bending line (34 mm). The numerical result of Von-Mises stress (A) presents the location of the highest stress concentration. Whereas, maximum principal stress (B) states the stress region that the initial crack can occur [66]. The simulation results define the highest stress concentration occurs at the edge of the fillet (A) and tension zone is the location where maximum principal stress occurs (B). Both results from the simulation are entirely consistent with the actual region of the crack during usage.

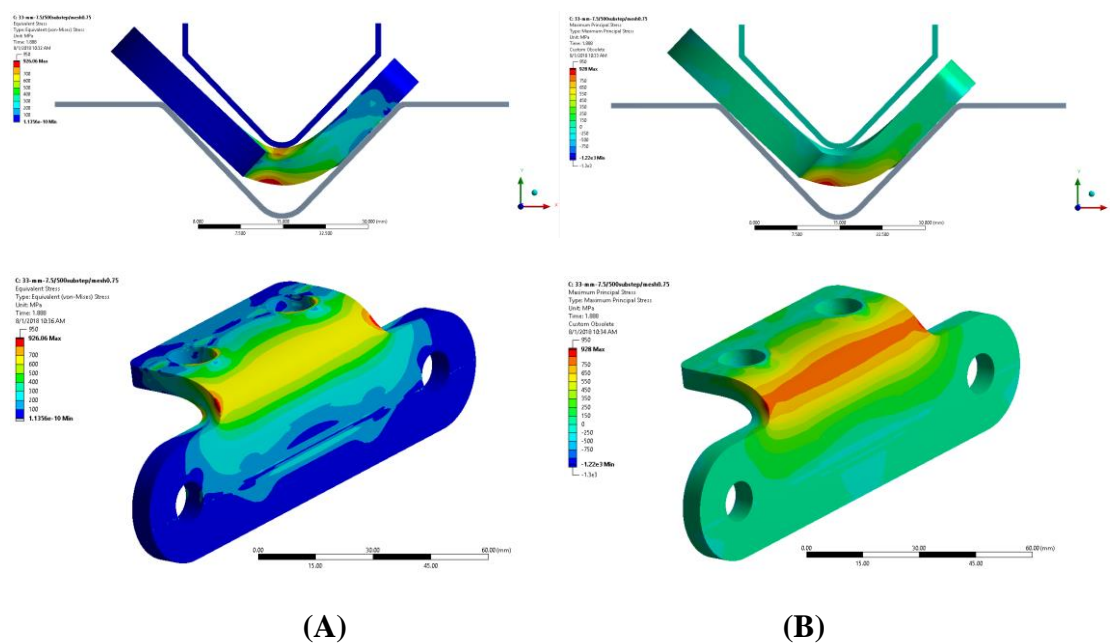


Figure 5.5 The Computer Simulation Result of PH-A (A) Von-Mises Stress, and (B) Maximum principal Stress

In this study, the new bending line 37 mm (PH-B) was examined in order to reduce the stress concentration on the fillet zone of the chain plate. Figure 5.6 presents that the new bending line effectively reduce stress concentration of the chain plate.

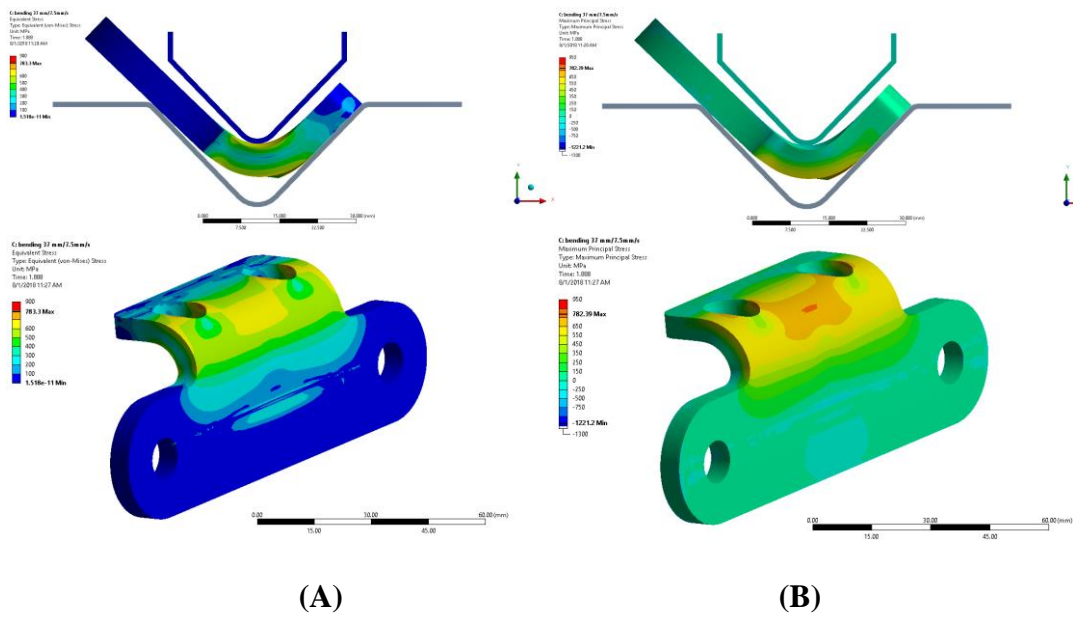


Figure 5.6 The Computer Simulation Result of PH-B (A) Von-Mises Stress, and (B) Maximum principal Stress

The results of this study are shown in Figure 5.7. The test results revealed that the stress concentration on the fillet zone of the original bending line (A) is higher than that of the new position (B). It can be seen that the stress distribution in the fillet zone of the new bending line has changed, thereby leading to a reduction in stress concentration and the cracking during usage. The results can be explained by the fact that the bending line has a significant influence on the stress concentration of the specimen.

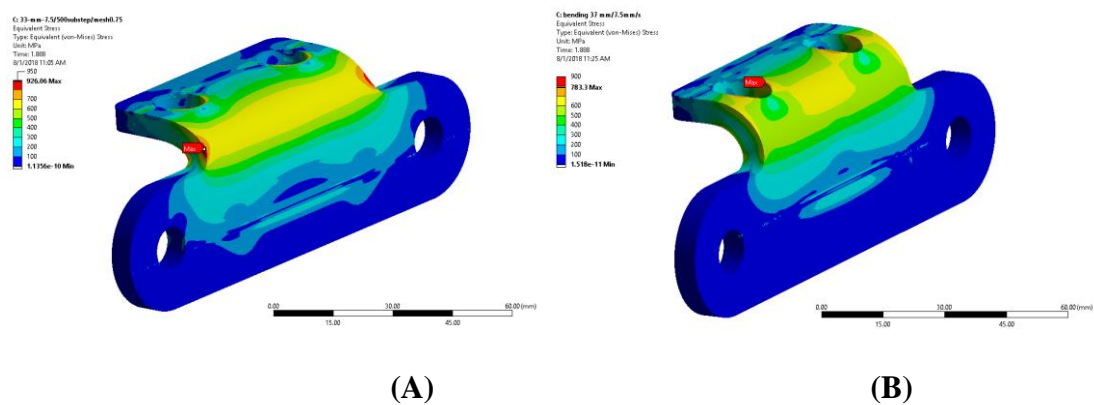


Figure 5.7 The Comparison between (A) The Original Bending line, and (B) The New Bending line

The measurement positions of the chain plate are shown in Figure 5.8. Position (A) was measured on the area that is perpendicular to the bending line to analyze stress distribution of the specimen and Position (B) was measured near the fillet zone to analyze the stress concentration at the corner of the fillet.

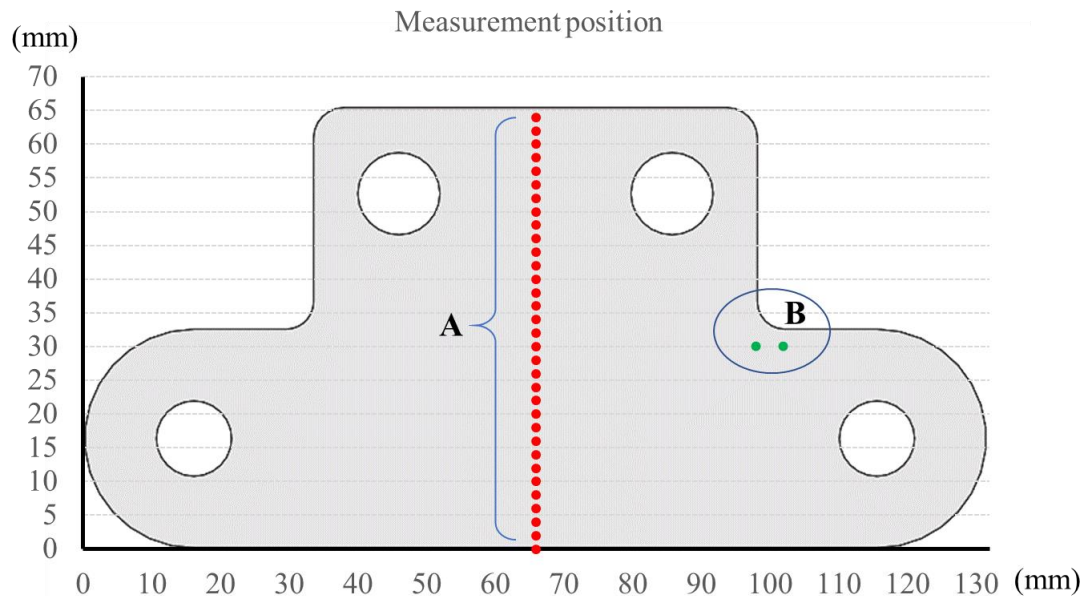


Figure 5.8 The Measurement Positions of the Specimen

Figure 5.9 presents Von-mises stress (A) and principle stress (B). PH-A represents the stress distribution of the original bending line. The results from the simulation indicated that the maximum stress region is at 36 mm which occurs in the fillet zone. Whereas, PH-B represents the stress distribution of the new bending line. The results showed that the maximum stress region has shifted from 36 mm to 42 mm. The simulation results revealed that the bending process design can prevent the high stress concentration at the corner of the fillet which lead to the formation of the cracking during usage.

The specimens were measured at the same position as shown Figure 5.11. The corner of the fillet and the fillet zone were analyzed to validate the stress concentration of the specimens.

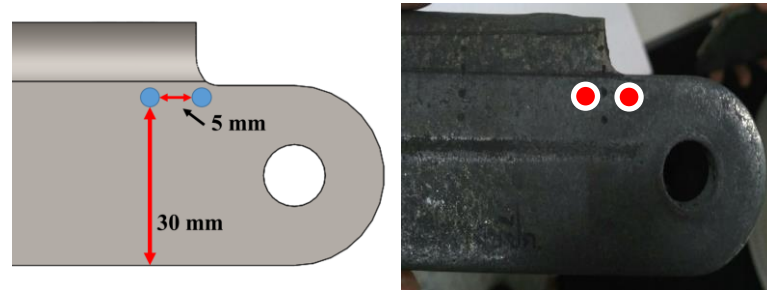


Figure 5.11 Validation of the Computer Simulation with Micro Vickers Hardness Test near the Fillet Zone

The hardness results at the fillet of the chain plate are shown in Table 5.5. The results of the bending simulation showed that the hardness was converted from equivalent stress to micro Vickers hardness. The simulation results are in accordance with the actual specimen measurement results. The hardness results of the new bending line (161.2 HV) is lower than the original bending line (205.7 HV). It can be seen that position 1 presents a higher hardness result than position 2. It was found that there was a higher effect on residual stress at position 1 due to the location of the fillet zone. This proves that the new bending line can effectively reduce the stress concentration on the fillet of the chain plate which leads to the formation of the cracking during usage.

Table 5.5 The Results from Vickers Hardness Test and Simulation

	Code	Micro Vickers Hardness Test (HV)	
		Position 1	Position 2
The original bending line	Specimen-A	205.7	177.4
	PH-A	185.82 (592 MPa)	160.29 (513 MPa)
The new bending line	Specimen-B	161.2	151.4
	PH-B	157.58 (501 MPa)	131.77 (447.27 MPa)

Figure 5.12 shows the hardness results of the specimens measured by micro Vickers hardness test. In comparison with the test results, the new bending line (b) presented lower hardness result than that of the original bending line (a). The hardness profile obtained from the simulation are entirely consistent with the actual region of stress distribution of the specimens.

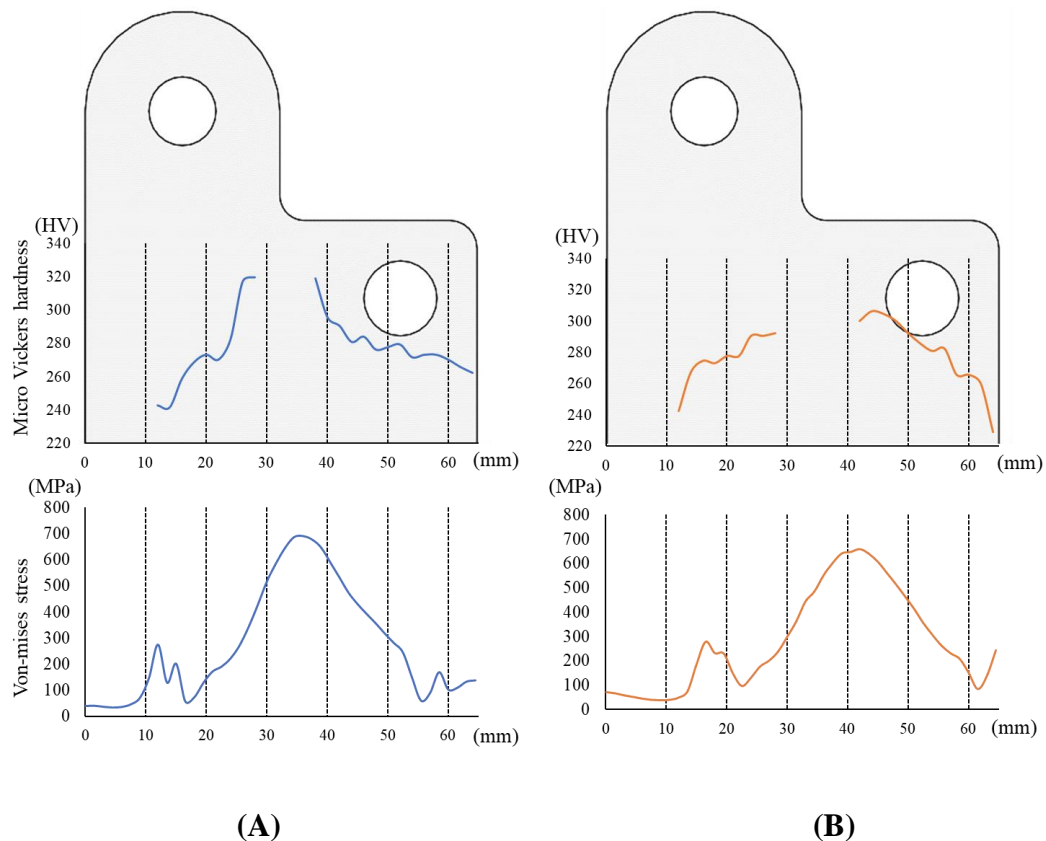


Figure 5.12 Validation between Computer Simulation Result and Lab Test of Specimen (A) the Original Bending line (34 mm) and (B) the New Bending line (37 mm)

The phenomena of the specimens after the bending process are shown in Figure 5.13 (the original bending line) and Figure 5.14 (the new bending line). The Figures present the deformation results of geometry and dimension of the specimen from computer simulation (A) and the bending machine (B).

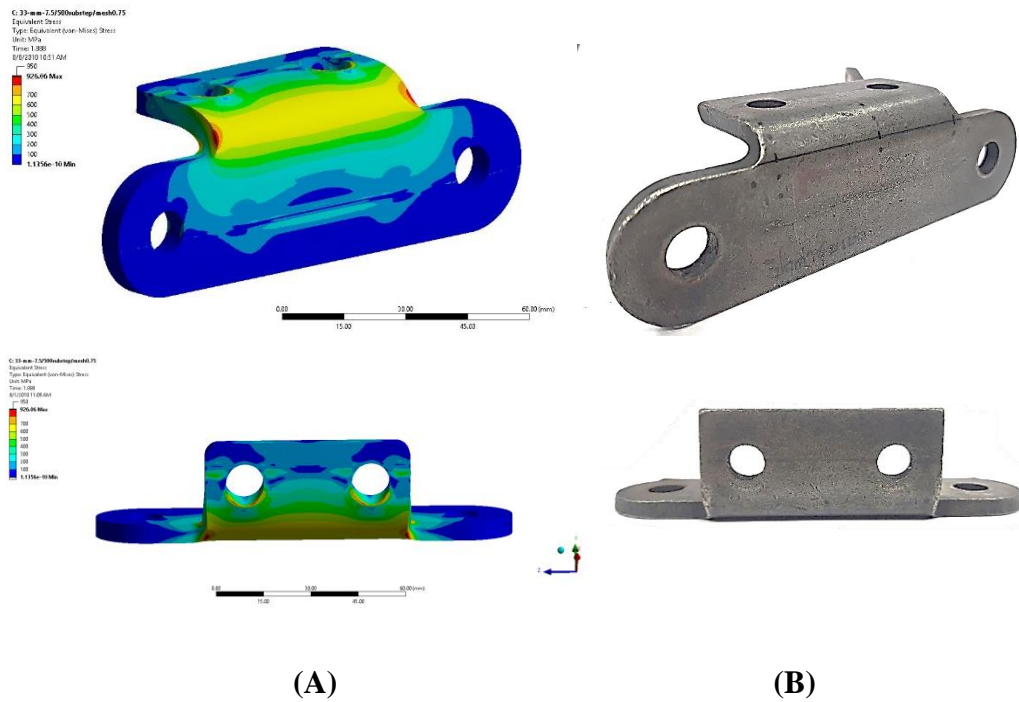


Figure 5.13 The Comparison of Bending Process Results between (A) the Computer Simulation, and (B) the Bending Machine (34 mm)

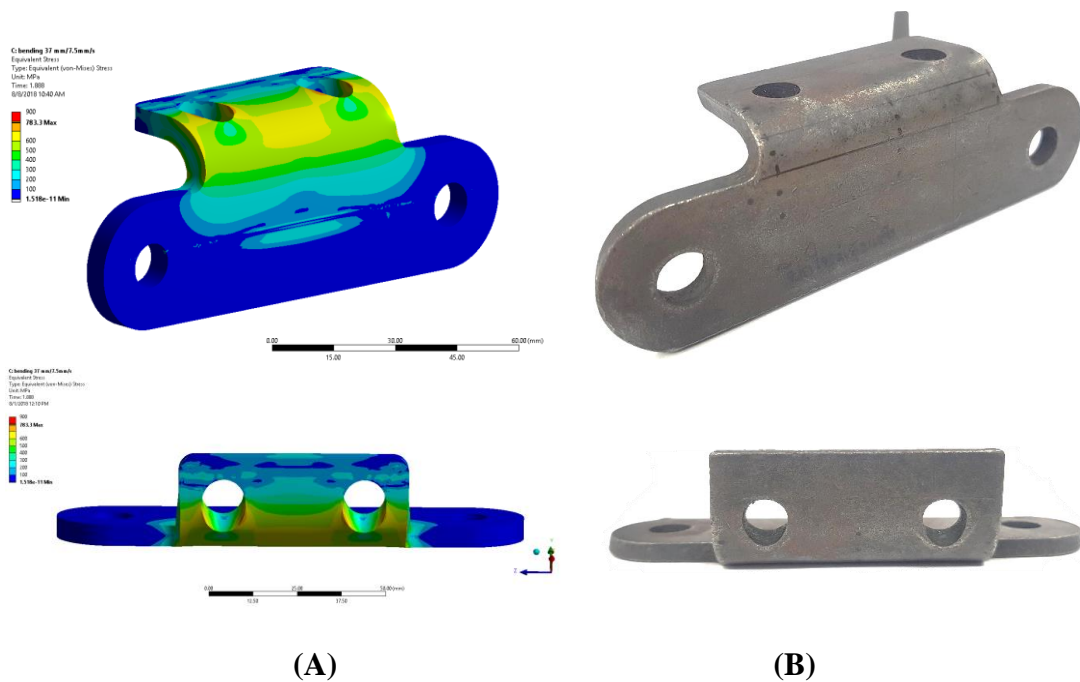


Figure 5.14 The Comparison of Bending Process Results between (A) the Computer Simulation, and (B) the Bending Machine (37 mm)

5.5. Discussion

The simulation results from the study defined the highest stress concentration occurred at the edge of fillet of the original bending line. The test results revealed that the simulation results are entirely consistent with the actual region of the cracking during usage. Therefore, the new bending line 37 mm was examined in order to reduce the stress concentration on the fillet zone of the chain plate. The results indicated that the stress concentration on the fillet zone of the original bending line is higher than that of the new bending line. The results stated that the stress distribution on the fillet zone of the new bending line had changed, thereby leading a reduction in stress concentration and the crack during usage. The micro Vickers hardness results proved that the bending process design can effectively reduce and prevent the high stress concentration on the fillet of the chain plate and results in the lifetime extension.

5.6. Future Work

The limitation in this part of the study is primarily concerned with high costs of raw materials and characterization methods. For further research using V-die bending process can be made as follows;

1. The analysis and investigation of the effect of corrosive seawater on the chain plate by using SEM and other techniques
2. The analysis of residual stress of the chain plate by XRD technique

Chapter 6 Conclusion

The first part of this thesis aimed to investigate and improve the surface hardness and wear resistance of the roller chain parts, which results in the chain lifetime extension. There are several factors affecting the quality of the roller chain parts in the heat treatment process.

Decarburization still occurs in the original heat treatment process of the factory, since only 20 grams of charcoal mixture charging in the begin cannot prevent the oxidation reaction during the whole process of heat treatment. Decarburization during the heat treatment process plays an important role in decreasing the surface hardness and wear resistance at the 50 micron-layer beneath the outside surface.

The results of the 11 mm pin from the experiment indicated that CB-02 and CN-01 specimen shows the best wear resistance. The results showed that the mechanical properties of the specimens from adding CB-02 and CN-01 presented nearly the same, although adding a lesser amount of hardening agent with the mixture of urea in CN-01. One possible reason can be that the hardening agent with the mixture of urea plays an important role in increasing the surface hardness of the specimens. The experiment also showed that the wear resistance ability in both cases improved approximately 50% or by double compared to that of the original product.

The experiment design of the 9.5 mm pin was carried out after considering the results from the 11 mm pin. The wear loss area of CN-30s was lower than the original product around 10-15%, which has no significant different from the original product. Whereas, CB-30 presented the best wear resistance ability, which was 30% higher than that of CN-30s.

The test results of the 5.9 mm pin indicated that the rise of the amount of hardening agent added into the furnace with the specimens improved the wear resistance ability of the pin part. The wear test results of the test specimen after 15 minutes showed better wear resistance than the original product around 50%. However, after 30 minutes, the test specimens showed almost the same values of the wear loss area whereas, the experiment results presented better wear resistance than the original product around 20%.

The experiments can be explained by the fact that the addition of the hardening agent with the specimens at the beginning of the process was not sufficient to improve the wear resistance ability of pin parts. As a result, the hardening agent was added with the specimens into the furnace and at the mid-point of the holding period to improve wear resistance. The results of the experiment from the addition of the hardening agent into the furnace to improve the wear resistance of the pin parts showed that the amount and the ratio of the hardening agent has a significant effect on the mechanical properties. The suitable amount of the hardening agent has a significant influence on mechanical properties of the specimens, thereby leading to an increased lifetime.

The second part of the thesis was to increase the lifetime of the chain plate in the corrosive condition. The computer simulation was used to examine in order to improve the bending process design and to prevent the high stress concentration at the corner which leads to the formation of the cracking during usage. The simulation results from the study defined the highest stress concentration occurred at the corner of the fillet in the original bending line (34 mm). The test results revealed that the simulation results are entirely consistent with the actual region of the crack during usage. The new bending line (37 mm) can reduce the stress concentration on the fillet zone of the chain plate. The simulation results which were validated with the micro Vickers hardness results proved that the bending process design can effectively reduce the high stress concentration and prevent cracking at the fillet of the chain plate which results in the lifetime extension.

This thesis offered the solutions that help the factory to improve the surface hardness and wear resistance of the roller chain parts by developing the heat treatment process and to prevent cracking during usage of the chain plate by using computer simulation to improve the bending process design. Both cases resulted in the lifetime extension of the roller chain used in an industrial factory and the agricultural industry.

Bibliography

[1] Standard Precision power transmission roller chain, attachment, and sprocket, 2011.

[2] Understanding wear life, Diamond Chain Company, Inc., <http://www.diamondchain.com/understanding-wear-life.php> (accessed online on 12/04/17).

[3] G.F. Vander Voort, *Advance materials & process*, February (2015) 22-27.

[4] T.V. Rajan, C.P. Sharma and A. Sharma, *Heat Treatment Principles and Techniques*, second edition, PHI Learning Private Limited, New Delhi (2011), 130 p.

[5] Sachio Shimura., *The Complete Guide to Chain*, Kogyo Chosakai Publishing Co., Ltd., 1997.

[6] William E. Bryson, *Heat Treatment Master Control Manual*.

[7] T. Senthilkumar, and T. K. Ajiboye, *Effect of Heat Treatment Processes on the Mechanical Properties of Medium Carbon Steel*, *Journal of Minerals & Materials Characterization & Engineering*, Vol. 11, No.2 pp.143-152, 2012.

[8] P. Poppy, S. Yudha, M. A. Muflich, A. Andoko, S. Sukarni, H. Suryanto *Hardness Improvement on Low Carbon Steel using Pack Carbonitriding Method with Holding Time Variation*, *Proceeding of the 6th Annual Basic Science International Conference* March 2016.

[9] F.O. Aramide, S.A. Ibitoyeb , I.O. Oladelea , J.O. Borode, *Effects of Carburization Time and Temperature on the Mechanical Properties of Carburized Mild Steel, Using Activated Carbon as Carburizer*, *Materials Research*, Vol. 12, No. 4, 483-487, 2009.

[10] F.O. Aramide, S.A. Ibitoyeb , I.O. Oladelea , J.O. Borode, Pack Carburization of Mild Steel, using Pulverized Bone as Carburizer: Optimizing Process Parameters, Leonardo Electronic Journal of Practices and Technologies ISSN 1583-1078 Issue 16, January-June 2010 p. 1-12.

[11] P.A. Ihom. Case hardening of mild steel using cow bone as energizer, African Journal of Engineering Research Vol. 1(4), pp. 97-101, October 2013.

[12] Compound for carbonitriding of articles made from alloyed steels, Russian patent no. 2314363, <http://russianpatents.com/patent/231/2314363.html> (accessed online on 10/11/16)

[13] N. Hagemann, K. Spokas, Hans-Peter Schmidt, Ralf Kägi, M.A. Böhler and Thomas D. Bucheli, Activated Carbon, Biochar and Charcoal: Linkages and Synergies across Pyrogenic Carbon's ABCs, Water 2018, 10, 182; doi:10.3390/w10020182.

[14] J. Pastor-Villegas, J.F. Pastor-Valle, J.M. Meneses Rodriguez, M. Garcia, Study of commercial wood charcoals for the preparation of carbon adsorbents, (2006) P103–108.

[15] Charcoal, <http://ukrfuel.com/news-chemical-properties-of-charcoal23.html> (accessed online on 12/04/17).

[16] George E. Totten, Ph.D., FASM, Steel Heat Treatment Metallurgy and technology.

[17] Harry Chandler, Heat Treater's Guide: Practices and Procedures for Irons and Steels.

[18] C. R. Sant Ana Filho, A. L. R. M. Rossete, C. R. O. Tavares, C. V. Prestes and J. A. Bendassolli, Sythesis of N-Enriched urea ($\text{CO}(\text{NH}_2)_2$) from NH_3 , CO , AND S in a discontinuous process, Vol. 29, No. 04, pp. 795 - 806, October - December, 2012

[19] Svetlana Bashkova, Teresa J. Bandosz, The effects of urea modification and heat treatment on the process of NO₂ removal by wood-based activated carbon, *Journal of Colloid and Interface Science* 333 (2009) 97–103

[20] Gas nitriding, <https://www.ald-france.eu/processes/nitriding/gas-nitriding> (accessed online on 12/04/17).

[21] Michael J. Schneider, Introduction to Surface Hardening of Steels, The Timken Company, and Madhu S. Chatterjee, Bodycote, ASM Handbook, Volume 4A.

[22] Olga Karabelchtchikova, Fundamentals of Mass Transfer in Gas Carburizing, November 2007

[23] D.A. Okongwu & V. Paranthaman, Assessment of the efficacy of some carbonate minerals as energizers in pack carburization of mild steel, *NIJOTECH VOL. 11. NO. 1* September 1987, P 28.

[24] George F. Vander Voort, Measurement of Decarburization of Heat-Treated Steel Surfaces, Consultant – Struers Inc., Wadsworth, Illinois USA, *Microsc. Microanal.* 20 (Suppl 3), 2014

[25] G.L. huyett, Engineering handbook technical information, 2004

[26] Geoffrey Parrish, Carburizing: Microstructures and Properties, p 37-49.

[27] Geoffrey Parrish, Carburizing: Microstructures and Properties p 77-97.

[28] George E. Totten, Steel Heat Treatment Metallurgy and Technologies,

[29] William D., Jr. Callister, Materials science and engineering, 7th edition 2007.

[30] Wolfgang Bleck (Hrsg.), Material Testing, Textbook for RWTH Students, 2007.

[31] Samuel R. Low, Materials science and Engineering Laboratory, January 2001.

-
- [32] Semih Genculu, P.E., Correlation of Hardness Values to Tensile Strength.
- [33] Elia E. LEVI, Hardness Testing Made Simple, 2003
- [34] James M. Gere, Mechanics of Materials sixth edition, 2004
- [35] ALI FATEMI, Mechanical Properties and Testing of Metallic Materials, The University of Toledo, Toledo, Ohio 43606, United States.
- [36] Wear mechanism, http://emrtk.unimiskolc.hu/projektek/adveng/home/kurzus/korsz_anyagtech/1_konzultacio_elemei/wear_and_wear_mechanism.htm
(accessed online on 5/11/18)
- [37] Ing. Ingrid Kovaříková, e.g., Study and Characteristic of Abrasive Wear Mechanism, Slovak research and Development Agency under the contract No APVV-0057-07, VEGA 1/0381/08, APVT-20-011004
- [38] V. K. Dodiya, J. P. Parmar, A Study of Various Wear Mechanism and its Reduction Method, International Journal for Innovative Research in Science & Technology| Volume 2 | Issue 09 | February 2016
- [39] A. Patnaik, R. K. Sharma, Parametric Optimization and Three-Body Abrasive Wear Behavior of Sic Filled Chopped Glass Fiber Reinforced Epoxy Composites Gaurav Agarwal, 2 International Journal of Composite Materials 2013
- [40] Standard Test Method for Wear Testing with a Pin-On-Disk Apparatus, May 2000.
- [41] William A. Glaeser, Wear-Resistant Hard Materials, 1997, P540.
- [42] Nadendla Srinivasababu, Wear Behavior of SAE 4340 Steel – Single Specimen, International Journal of Modern Trends in Engineering and Research e-ISSN No.:2349-9745, Date: 2-4 July, 2015.
- [43] Ivan sachy, Handbook of die design second edition, 2006.

[44] Amul Biradar, M.D Deshpande, Finite Element Analysis of Spring back of a Sheet Metal in Wipe Bending Process, International Journal of Science and Research (IJSR) ISSN (Online): 2319-7064.

[45] Onur Turgay Sarikaya, Analysis of heat treatment effect on spring back in V-bending, november 2008.

[46] Stress concentration, https://www.engineersedge.com/material_science/stress_concentration_fundamentals_9902.htm (accessed online on 12/03/18).

[47] Walter D. Pilkey Peterson's, Stress concentration factors, Second Edition, 1997.

[48] Dheeraj Gunwant, Rahul Kshetri, Kamal Singh Rawat, Determination of Stress Concentration factor in Linearly Elastic Structures with Different Stress-Raisers Using FEM, journal of Engineering Research and Application, Vol. 6, Issue 2, (Part - 6) February 2016, pp.29-35.

[49] Emad Al-Momani, Ibrahim Rawabdeh, An Application of Finite Element Method and Design of Experiments in the Optimization of Sheet Metal Blanking Process, Jordan Journal of Mechanical and Industrial Engineering, Volume 2, Number 1, Mar. 2008

[50] Shephard, M. S., Beall, M.W., O'Bara, R.M. and Webster, B.E., "Toward simulation-based design," Finite Elements in Analysis and Design, pp. 1575- 1598, 2004.

[51] Esat V., Ms Thesis "Finite Element Analysis of Bending", 2002.

[52] A. Schey J., Introduction to Manufacturing Processes, 2nd Ed., McGrawHill Book Company, Inc., 1987.

[53] C. Maranh o and J. P. Davim, Residual Stresses in machining using Analysis, February 23, 2012

[54] Russell H. Jones, Stress-Corrosion Cracking Materials Performance and Evaluation, editor, p 1-40

[55] Stress corrosion cracking, <http://www.npl.co.uk/science-technology/advanced-materials/national-corrosion-service/publications/corrosion-guides> (accessed online on 20/05/18).

[56] R.A. Barros, H.L. Rodrigues, A.J. Abdalla, Evolution of sliding wear of bronze-aluminium 630 alloy in contact with AISI 4340 steel in different microstructural condition, Proc. of the 22nd International Congress of Mechanical Engineering (COBEM 2013), November 3-7, 2013.

[57] Manus satidjinda, Iron & Steel Heat-Treatment Engineering, June 1992, P 112

[58] Standard Method for Chemical Analysis of Wood Charcoal, 1990

[59] J.R. Davis, Davis & Associates, Surface Hardening of Steels Understanding the Basics, 2002

[60] Iron carbon phase diagram, http://www.substech.com/dokuwiki/doku.php?id=iron-carbon_phase_diagram (accessed online on 12/11/18)

[61] T.V. Philip, T.J. McCaffrey. Ultrahigh-Strength Steels, Metals Handbook, ASM International, (1990) pp. 430-434.

[62] W.S. Lee, T.T. Su, Journal of Materials Processing Technology 87 (1999) 198–206.

[63] D.H. Jeong, U. Erb, K.T. Aust, G. Palumbo, The relationship between hardness and abrasive wear resistance of electrodeposited nanocrystalline Ni–P coatings, Scripta Materialia 48 (2003), pp. 1067–1072.

[64] Mazdoor Kisan Shakti Sangathan, Jawaharlal Nehru, Indian Standard, Method of measuring decarburized depth of steel, 2000.

[65] P. Iglesias, M.D. Bermudez, W. Moscoso, B.C. Rao, M.R. Shankar, S. Chandrasekar, Friction and wear of nanostructured metals created by large strain extrusion machining, *Wear* 263 (2007), pp. 636-642.

[66] C. Maranhão and J. P. Davim, Residual stresses in machining using FEM- A review, *Rev.Adv.Master.Sci.* 30 (2012) 267-272.

Biography

PERSONAL INFORMATION

Name: Perawat Thongjitr

Date of Birth: 14/10/1992

Place of Birth: Bangkok, Thailand

Nationality: Thai

Address: 80/17 Soi Itsaraphab 23 Itsaraphab Rd., Bangkokyai Bangkok
10600

Campus Address: TGGs, KMUTNB Campus 1518 Pracharat 1 Rd., Wongsawang
Bangkok 10800

Tel.: +668 4700 7307

Email: perawat.t-mpe2015@tggs-bangkok.org

EDUCATION

2015-Present Studying Master of Materials and Production Engineering
(Metal Track) at TGGs, KMUTNB

2011-2014 Bachelor of Engineering (Mechanical Engineering) at
Rajamangala University of Technology Phra Nakhon (RMUTP)

2008-2010 High school at Taweethapisek school

EXPERIENCE

Student internship at Thai Airways International Public Co., Ltd.

Period of time: 6/11/2013 - 28/2/2014

Student internship at Thai Metro Industry (1973) Co., Ltd.

Period of time: 1/8/2016 - 10/12/16

CONFERENCE

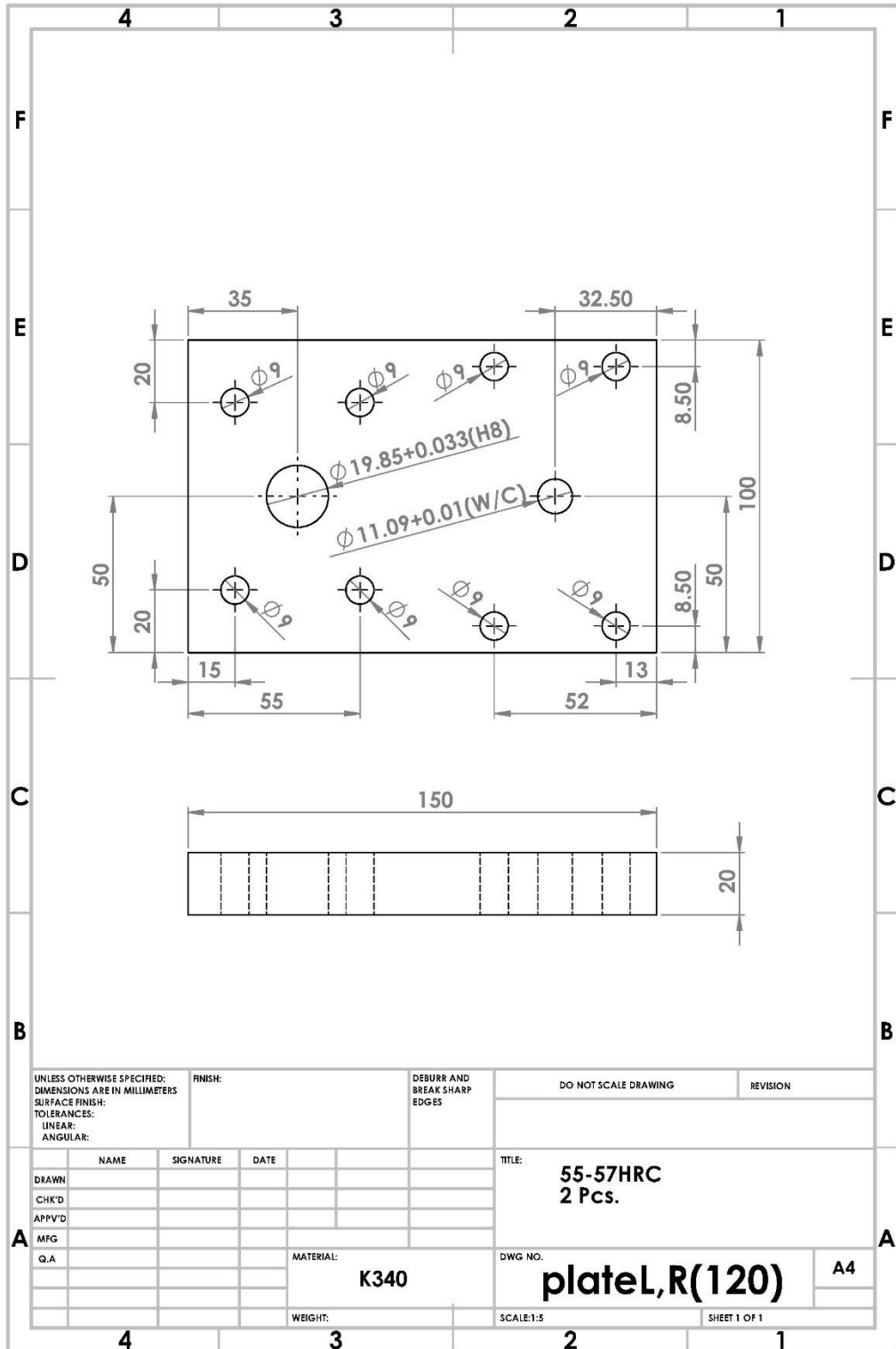
P. Thongjitr, P. Ninpetch, P. Kowitwarangkul, “Wear resistance improvement of the roller chain at Thai Metro Industry (1973) Co., Ltd.”, Materials Today: Proceedings 5 (2018) 9431–9439.

The 10th Thailand International Metallurgy Conference (The 10th TIMETC)
Ramada Plaza Bangkok Menam Riverside, Bangkok

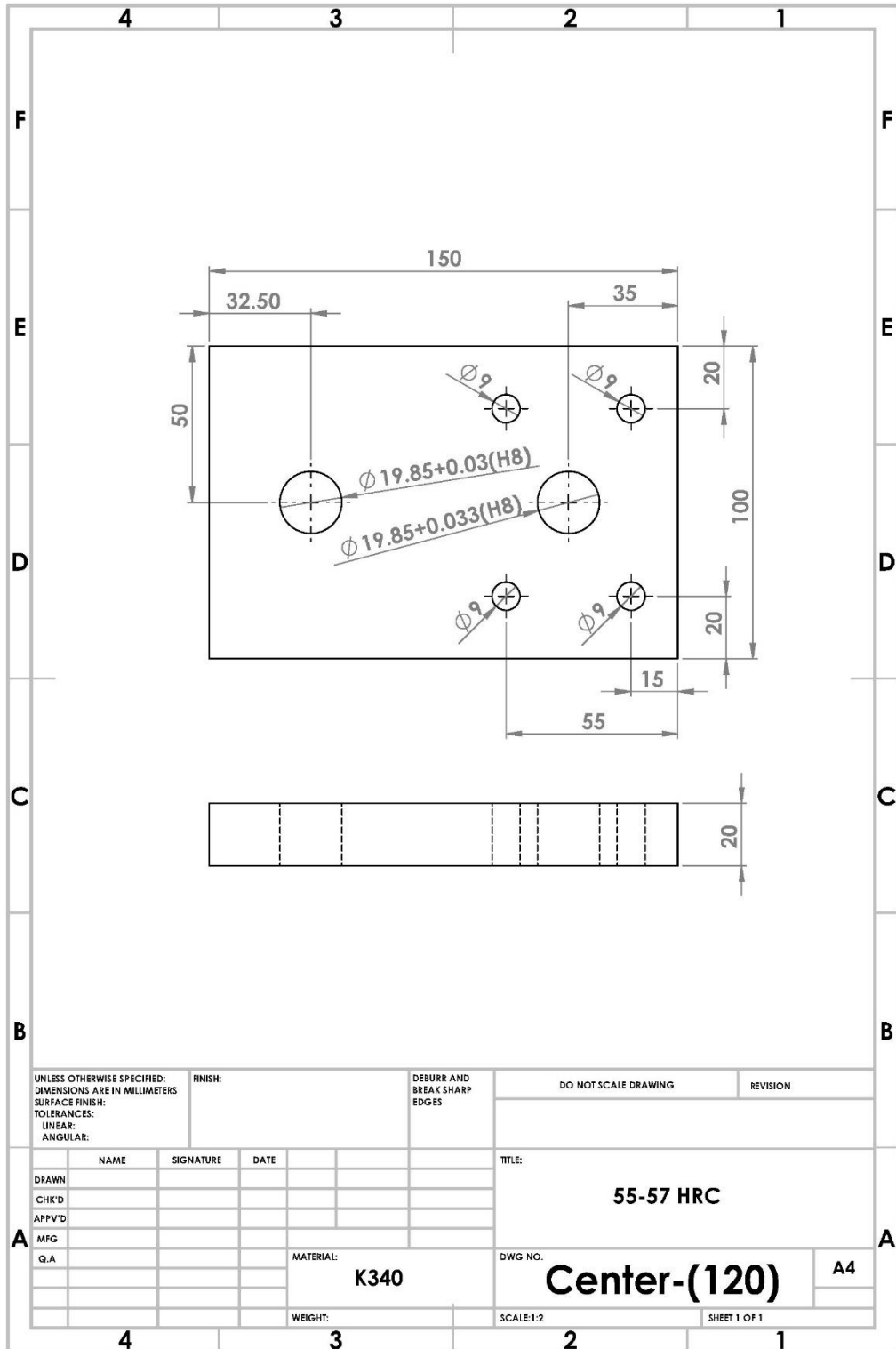
Period of time: 30/3/2017-31/3/2017

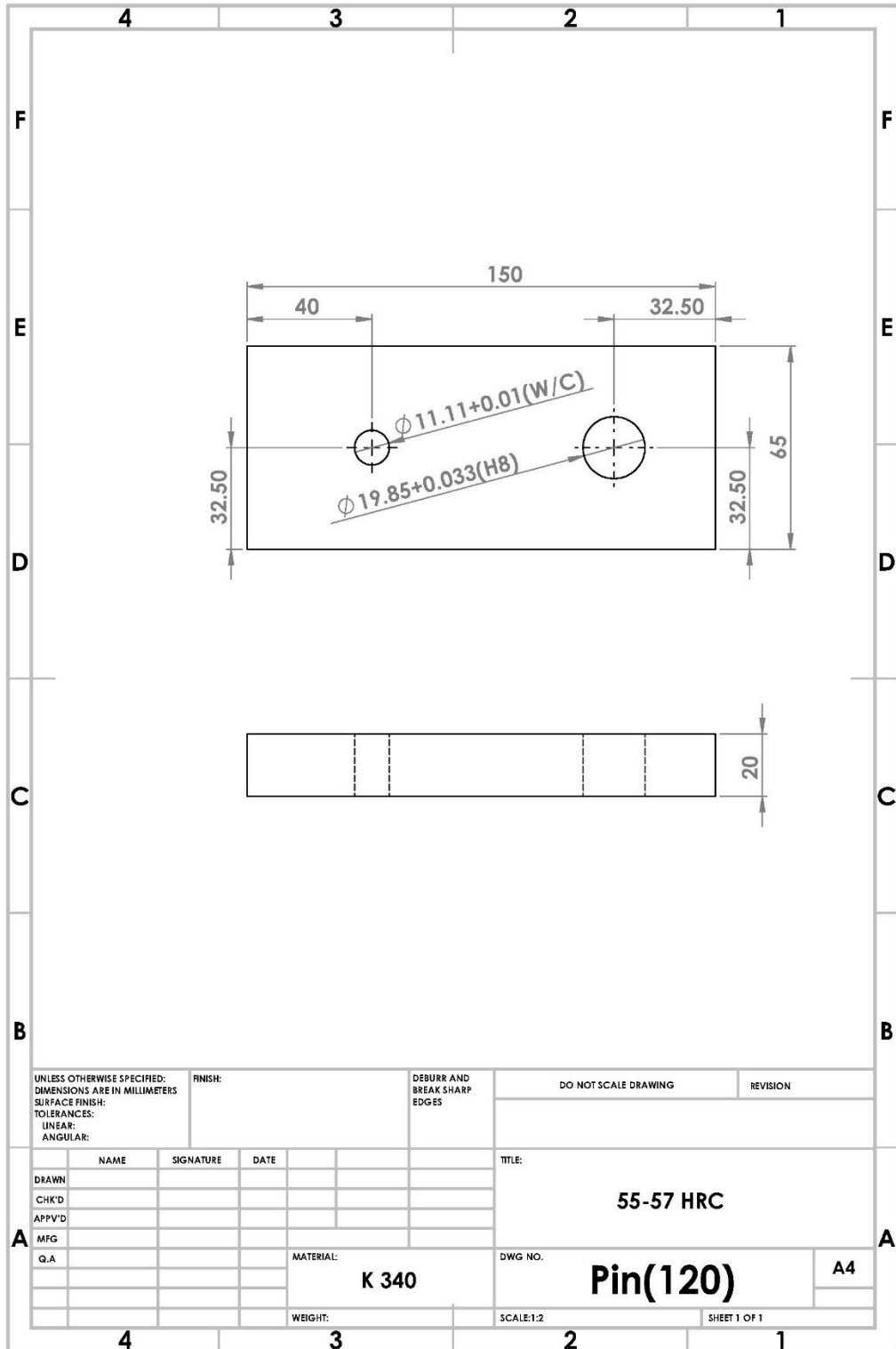
Appendix A

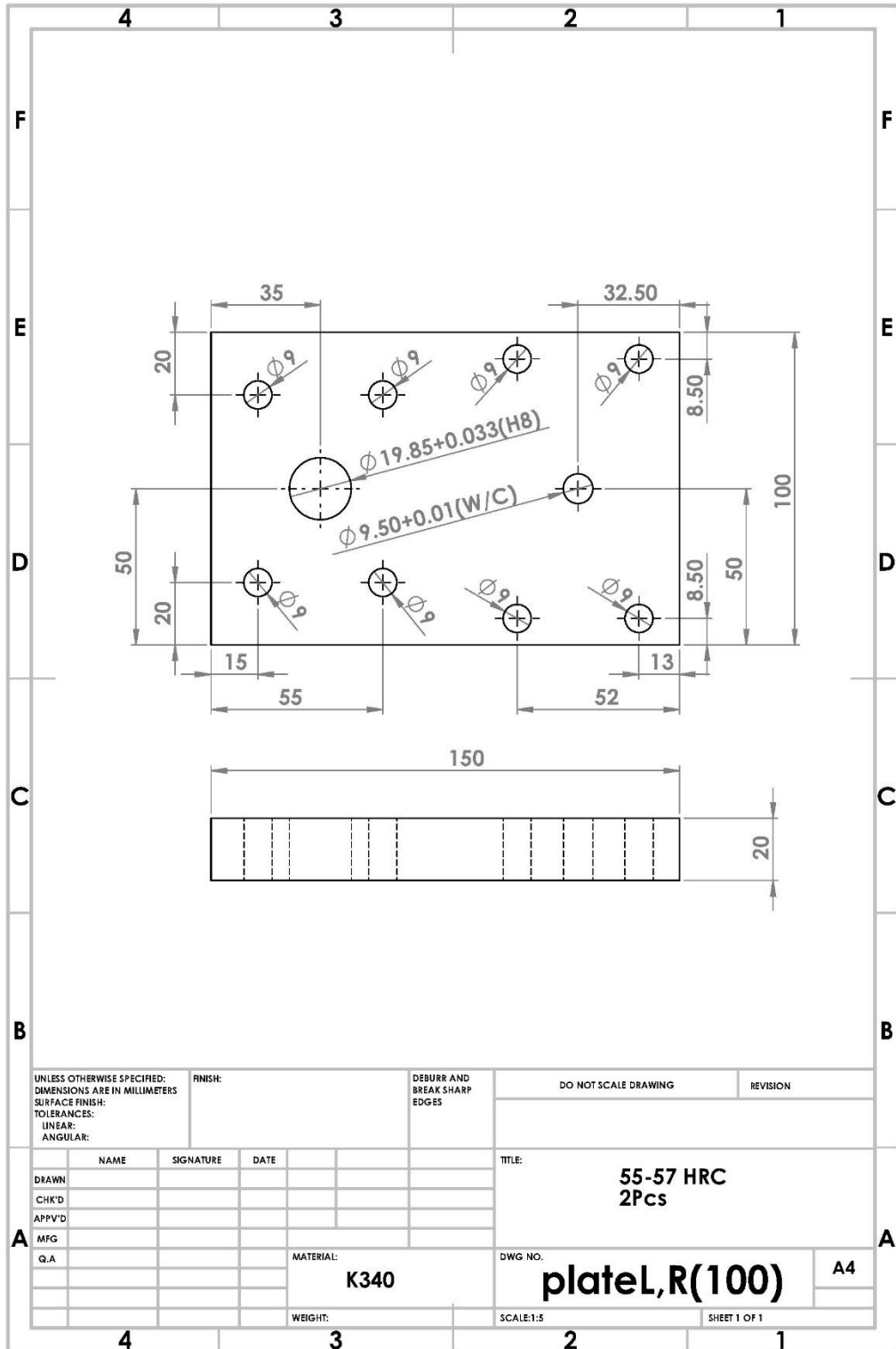
Part of assembly jig for double shear test



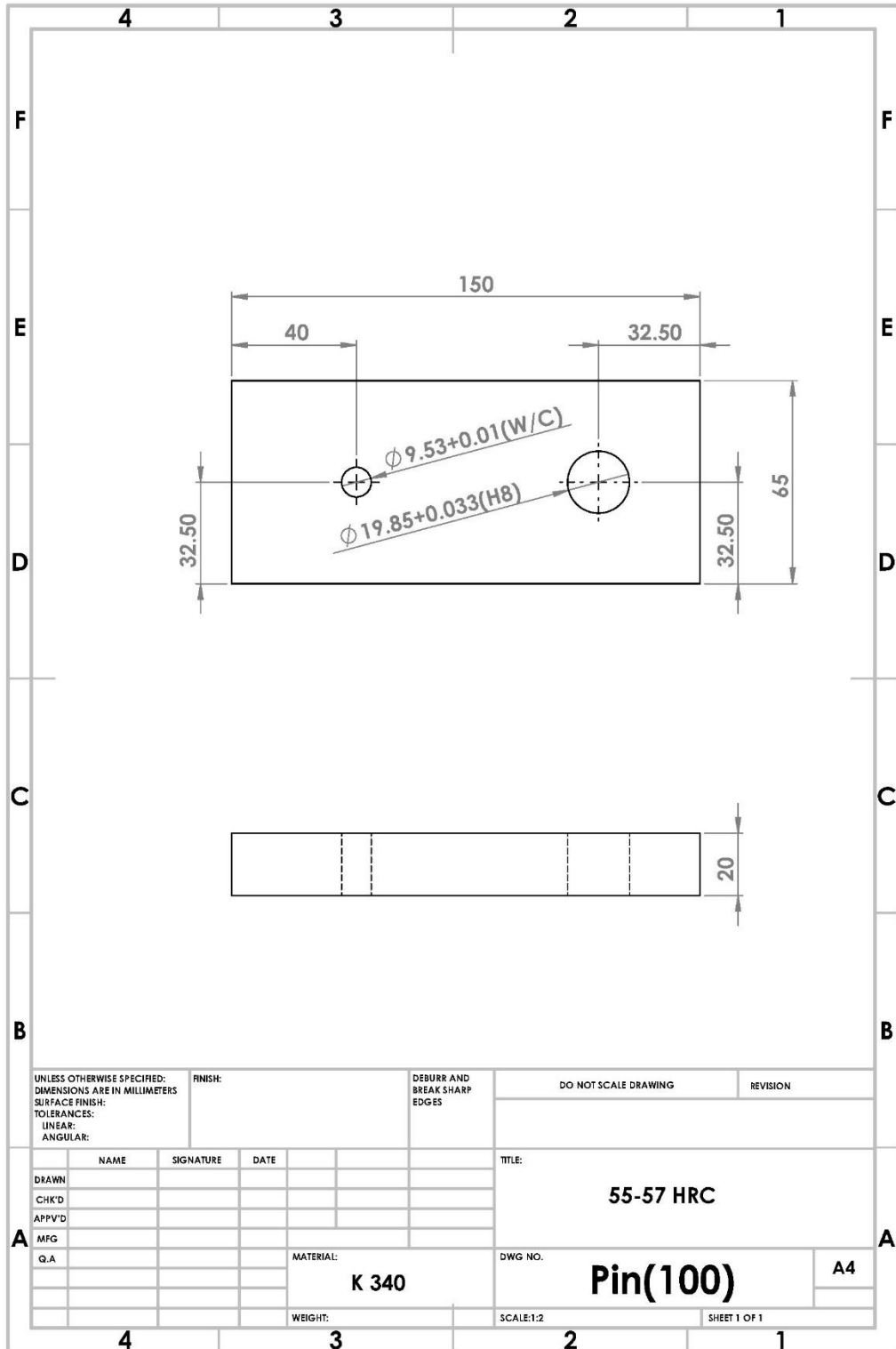
UNLESS OTHERWISE SPECIFIED: DIMENSIONS ARE IN MILLIMETERS		FINISH:		DEBURR AND BREAK SHARP EDGES		DO NOT SCALE DRAWING		REVISION	
SURFACE FINISH:									
TOLERANCES:									
LINEAR:									
ANGULAR:									
DRAWN		NAME	SIGNATURE	DATE	TITLE: 55-57HRC 2 Pcs.				
CHK'D									
APPV'D									
MFG					MATERIAL: K340		DWG NO. plateL,R(120)		A4
Q.A					WEIGHT:		SCALE:1:5		SHEET 1 OF 1

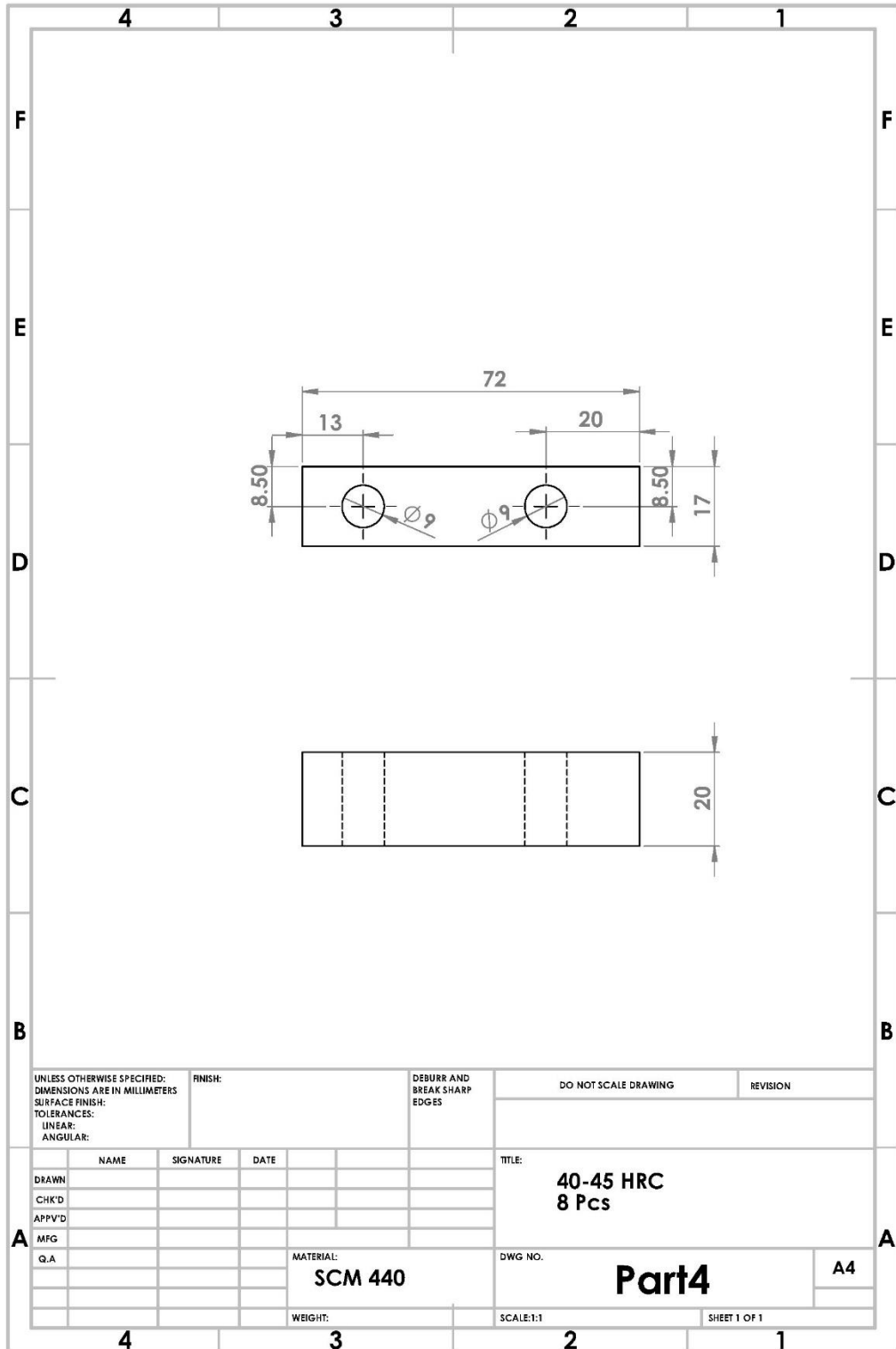




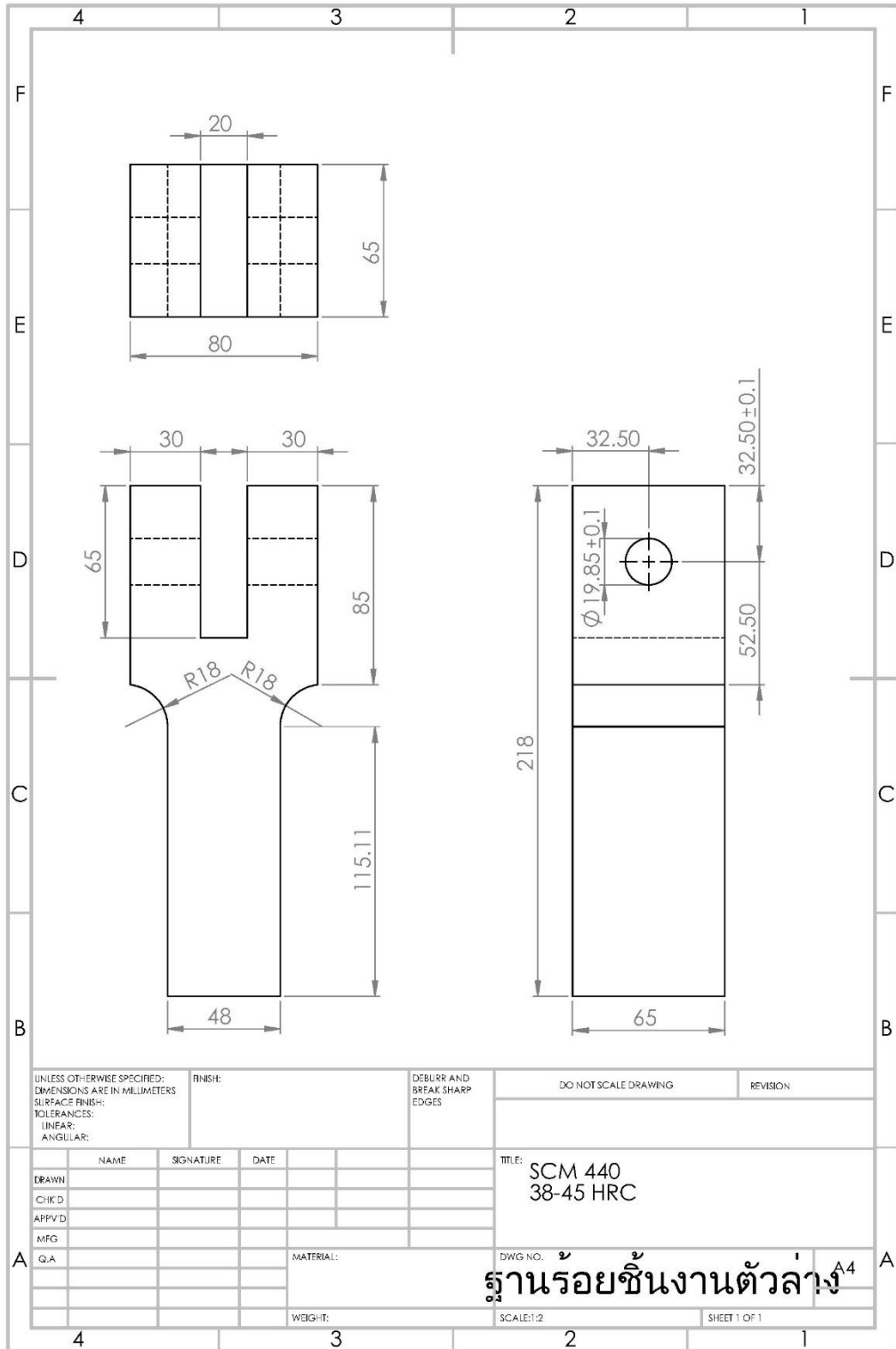


UNLESS OTHERWISE SPECIFIED: DIMENSIONS ARE IN MILLIMETERS SURFACE FINISH: TOLERANCES: LINEAR: ANGULAR:			FINISH:	DEBURR AND BREAK SHARP EDGES	DO NOT SCALE DRAWING	REVISION
NAME	SIGNATURE	DATE			TITLE: 55-57 HRC 2Pcs	
DRAWN					DWG NO. plateL,R(100)	
CHK'D					A4	
APPV'D					SCALE:1:5 SHEET 1 OF 1	
MFG				MATERIAL: K340		
Q.A				WEIGHT:		





UNLESS OTHERWISE SPECIFIED: DIMENSIONS ARE IN MILLIMETERS		FINISH:		DEBURR AND BREAK SHARP EDGES		DO NOT SCALE DRAWING		REVISION	
SURFACE FINISH:									
TOLERANCES:									
LINEAR:									
ANGULAR:									
NAME		SIGNATURE		DATE		TITLE:			
DRAWN						40-45 HRC			
CHK'D						8 Pcs			
APPV'D									
MFG						DWG NO.		A4	
Q.A						MATERIAL:		Part4	
						SCM 440			
						WEIGHT:		SCALE:1:1	
								SHEET 1 OF 1	



UNLESS OTHERWISE SPECIFIED: DIMENSIONS ARE IN MILLIMETERS		FINISH:		DEBURR AND BREAK SHARP EDGES		DO NOT SCALE DRAWING		REVISION	
SURFACE FINISH:									
TOLERANCES:									
LINEAR:									
ANGULAR:									
DRAWN		NAME	SIGNATURE	DATE	TITLE: SCM 440 38-45 HRC				
CHK'D									
APPV'D									
MFG									
Q.A		MATERIAL:			DWG NO.		ฐานรอยชิ้นงานตัวล่าง A4		
		WEIGHT:			SCALE: 1:2		SHEET 1 OF 1		

Appendix B

Example of double shear test result



Thai-German Institute
สถาบันไทย-เยอรมัน

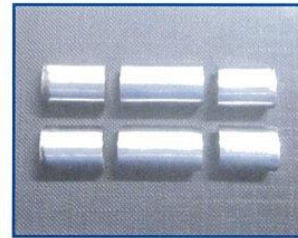
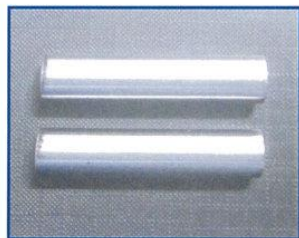
สถาบันไทย-เยอรมัน 700/1 หมู่ที่ 1 นิคมอุตสาหกรรมอมตะนคร ถนนพหลโยธิน-ตราด กม.57 ตำบลคลองลำทุบ อำเภอเมืองจังหวัดชลบุรี 20000
Thai-German Institute 700/1 Moo.1 Amatanakron Industrial Estate Bangna-Trad KM.57 Tambol Klomng Lam Tu B Amphur Muang Chonburi 20000
Tel. 038-215033-44 Fax. 038743705 http://www.tgi.or.th

TEST REPORT

Received No. : 59-12-078
Report No.:TGI-TS-001
Rev.: 00

Customer's company name : **Thai Metro Industry (1973) Co., Ltd.**
Address: **47 Moo 4 Puchosamingprai Rd., T.Bangpong, A.Muang, Samuthprakarn 10270**

Product Name:	PIN ชุดใส่ 11 มม.	Material Characterization:	-
Part Name:	C-01	Standard of Test:	-
Part No.:	-	Test Method:	Shear Test
Material Specification:	-	Type of Test:	Tensile Testing
Received Date:	20 / Dec. / 2016	Equipment / Serial No.:	Universal Testing Machine
Tested Date:	20 / Dec. / 2016	Equipment's Capacity:	Tension force 100 Tons
		Ambient Temp.:	22.7 °C, 55 % RH



Result of Shearing Test

Test No.	Diameter (mm)	Area x 2 (mm ²)	Max. Load (kN)	Max. Load (kgf)	Shear Strength (N/mm ²)
TS-001	11.07	192.50	208.773	21,288.990	1,084.535
TS-002	11.07	192.50	206.877	21,092.707	1,074.685

Operated by: *Sutzaorn* Checked by: *JA* Approved by: *JA*
 Testing Operator Mr.Arun Jeangsrijaroen Mr.Arun Jeangsrijaroen
 Technical Team Technical Manager Quality Manager
 (20 / Dec. / 2016) (20 / Dec. / 2016) (20 / Dec. / 2016)

Commentary:

1. Our division and institute not allow to change, add or subtract anywhere on this report, except only in case of already accepted by writing from our division.
2. Our division can not confess to any direct or indirect damage that will occur after this by using data, analysis results, results or conclusion in this report to design, produce or others.
3. Experiment results are exactly true especially only on specimen that was carried to test.
4. "Test marked * in this report are not included in the TISI Accreditation Schedule for our Laboratory"



Thai-German Institute
สถาบันไทย-เยอรมัน

TENSILE TEST

Customer's Company Name : **Thai Metro Industry (1973)**

Test Object : **C-01**

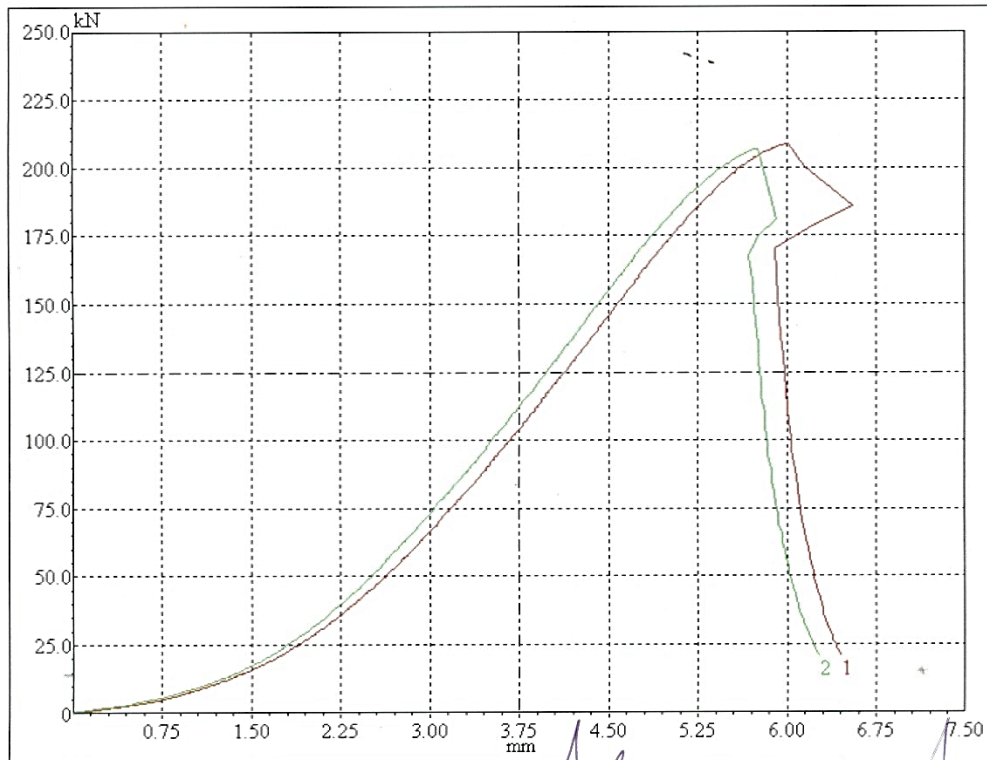
Material Specification : -

Testing Date : **20-12-2016**

Received No. : **58-06-XX**

Report No. : **TGI-TS-001**

Test No.	Diameter mm	Area mm ²	Max Load kN	Max Load kgf
1	11.07	96.25	208.773	21288.990
2	11.07	96.25	206.877	21095.707



Tested By : *Sitz. (for)*
Testing Operator
Technical Team

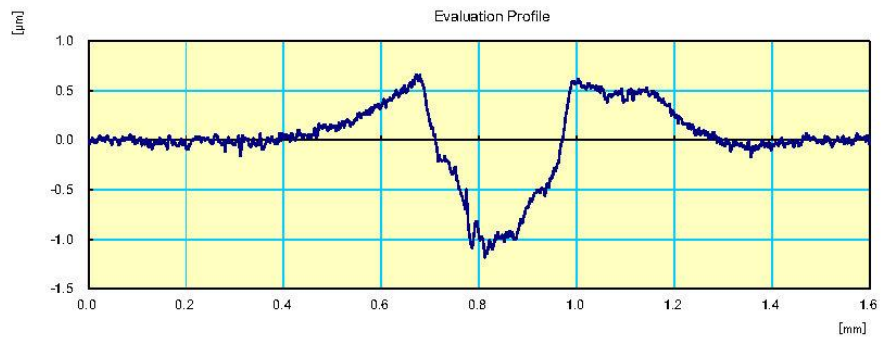
Tested By : *J. Komou*
Ms. Kamonwan Komou
Technical Manager

Approved By : *A. Jeangsrijaoen*
Mr. Arun Jeangsrijaoen
Quality Manager

Appendix C

Example of surface roughness result

CERTIFICATE OF INSPECTION



Work Name	Sample	Operator	Mitutoyo
Measuring Tool	SurfTest	Comment	Ver2.00
Standard	ISO 1997	N	2
Profile	R	Cut-Off	0.8mm
λs	2.5µm	Filter	GAUSS
Ra	0.242 µm	Rmr(c)2	17.375 %
Rq	0.363 µm	Rdc	0.291 µm
Rz	1.773 µm	Rt	1.844 µm
Rp	0.640 µm	Rz1max	1.797 µm
Rv	1.133 µm	Rk	0.242 µm
Rsk	-0.807	Rpk	0.523 µm
Rkµ	4.704	Rvk	1.079 µm
Rc	E0110 µm	Mr1	27.813 %
RSm	E0110 µm	Mr2	83.156 %
RDq	0.021	A1	7.27
Rmr	2.906 %	A2	9.09
Rmr(c)1	10.375 %		